Th1 effector T cells selectively orchestrate cardiac fibrosis in nonischemic heart failure

Tania Nevers,[1] Ane M. Salvador,[1] Francisco Velazquez,[1] Njabulo Ngwenyama,[1] Francisco J. Carrillo-Salinas,[1] Mark Aronovitz,[2] Robert M. Blanton,[2] and Pilar Alcaide[1]

[1]Sackler School of Graduate Biomedical Sciences, Tufts University School of Medicine, Boston, MA
[2]Molecular Cardiology Research Institute, Tufts Medical Center, Boston, MA

Despite emerging data indicating a role for T cells in profibrotic cardiac repair and healing after ischemia, little is known about whether T cells directly impact cardiac fibroblasts (CFBs) to promote cardiac fibrosis (CF) in nonischemic heart failure (HF). Recently, we reported increased T cell infiltration in the fibrotic myocardium of nonischemic HF patients, as well as the protection from CF and HF in TCR-$\alpha^{-/-}$ mice. Here, we report that T cells activated in such a context are mainly IFN-γ^{+}, adhere to CFB, and induce their transition into myofibroblasts. Th1 effector cells selectively drive CF both in vitro and in vivo, whereas adoptive transfer of Th1 cells, opposite to activated IFN-$\gamma^{-/-}$ Th cells, partially reconstituted CF and HF in TCR-$\alpha^{-/-}$ recipient mice. Mechanistically, Th1 cells use integrin α4 to adhere to and induce TGF-β in CFB in an IFN-γ–dependent manner. Our findings identify a previously unrecognized role for Th1 cells as integrators of perivascular CF and cardiac dysfunction in nonischemic HF.

INTRODUCTION

Heart failure (HF) is a chronic cardiac syndrome that results in a mean survival of 5 yr after diagnosis, currently placing more than 25 million people worldwide at risk of death. HF arises generally from the process termed pathological cardiac remodeling, in which the left ventricle (LV) and other cardiac chambers undergo progressive structural and functional abnormalities in response to pathological stress (Braunwald, 2013). Cardiac fibrosis (CF) represents one such structural change that occurs in the remodeled LV. Although originally thought to represent only a marker of adverse remodeling, CF has increasingly been identified to contribute to further LV functional deterioration during cardiac remodeling. CF arises when cardiac fibroblasts (CFBs), a prevalent resident cell type in the heart, become activated and transform into myofibroblasts, which in turn deposit fibrillary extracellular matrix (ECM) proteins in the myocardium, promoting adverse effects in cardiac structure and function (Fan et al., 2012). Further, although HF and cardiac remodeling arise from multiple and varied stimuli, such as pressure overload, infarction, autoimmune disease, toxins, and genetic mutations, CF generally occurs as a common final pathway regardless of the stimulus. Therefore, understanding the molecular and cellular triggers contributing to the CFB-myofibroblast transition may identify important mechanisms regulating pathological fibrosis in HF. T cells in particular have recently emerged as likely contributing to CF (Travers et al., 2016). However, the direct actions of T cells on the CFB are largely unexplored. Several studies have recently identified a critical role for T cells in cardiac repair after ischemia, where the fibrotic response functions as a protective process to heal and repair the area of injury. This healing response orchestrated by T cells is thought to be mediated by various immune cells, including monocytes, neutrophils, and macrophages, that are recruited to the site of ischemic injury in the heart (Frangogiannis et al., 2002; Hofmann et al., 2012), rather than by direct actions of the T cells on the CFB, the major source of ECM proteins. In contrast, in nonischemic HF, CF develops progressively as the CFB converts to profibrotic myofibroblasts in a pathological process to compensate for pressure overload and provokes changes culminating in cardiac dysfunction and HF (Fan et al., 2012). We previously reported that end-stage nonischemic HF patients have increased LV fibrosis directly associated with T cell infiltration (Nevers et al., 2015). Despite extensive investigation into the pathogenesis of T cell–mediated profibrotic cardiac repair after ischemia, little is known about the contribution of T cells to CF once HF is established in a pressure-overloaded heart, or the specific T cell subsets involved and the mechanisms that regulate CFB transformation and pathological CF.

In an effort to investigate the T cell–mediated mechanisms responsible for CF in nonischemic HF, we have adopted the mouse model of thoracic aortic constriction (TAC), which induces CF and nonischemic HF in response to LV pressure overload comparable to what is observed

Correspondence to Pilar Alcaide: Pilar.Alcaide@tufts.edu

Abbreviations used: AT, adoptive transfer; CF, cardiac fibrosis; CFB, cardiac fibroblast; ECM, extracellular matrix; FBM, fibroblast culture media; HF, heart failure; LV, left ventricle; LVEDP, left ventricular end diastolic pressure; MHC, myosin heavy chain; mLN, mediastinal LN; TAC, transverse aortic constriction.

The Rockefeller University Press
J. Exp. Med. 2017 Vol. 214 No. 11 3311–3329
https://doi.org/10.1084/jem.20161791

in patients with HF (Rockman et al., 1991; Patten et al., 2008; Blanton et al., 2012). In this setting, we and others have previously reported that $CD4^+$ T cells are activated in the cardiac draining LNs (mediastinal LNs [mLNs]), are recruited to the LV, and function as potent drivers of progressive fibrosis, because mice deficient in T cells (TCR-$\alpha^{-/-}$) and specifically in $CD4^+$ T cells (MHC-$II^{-/-}$) do not develop CF in response to TAC (Laroumanie et al., 2014; Nevers et al., 2015). Thus, these studies point to $CD4^+$ T cells as an important immune cell type influencing CF. However, mechanistically, whether T cells activated in the setting of pressure overload–induced HF can directly cross talk with the CFB, the specific $CD4^+$ T cell subset involved in the fibrotic outcome in HF, and the mechanisms by which this may occur, remain unknown. Th1-mediated immune responses typically involve the secretion of the cytokines IFN-γ, TNF-α, and IL-2. Intriguingly, the role of Th1 cytokines in contributing to fibrosis is controversial depending on the tissue (Gurujeyalakshmi and Giri, 1995; Oldroyd et al., 1999). In the heart, in the context of ischemia or angiotensin II infusion, IFN-γ–producing T cells have also been shown to regulate the differentiation and activation of macrophages, subsequently leading to inflammation and CF (Han et al., 2012; Hofmann et al., 2012). In contrast, IFN-γ protects from CF in autoimmunity (Afanasyeva et al., 2004; Fairweather et al., 2004). We have previously shown that IFN-γ and T-bet, the signature cytokine and transcription factor for Th1 cells, are significantly increased in the LV after 4 wk of TAC in WT C57BL/6 mice, and these are blunted in the TCR-$\alpha^{-/-}$ mice (Nevers et al., 2015), suggesting that IFN-γ–producing T cells play a pathogenic role in TAC-induced HF. Thus, paradoxically, the role of IFN-γ in CF is controversial and seems to depend on the type of disease modeled, and the mechanisms of action remain elusive. On the other hand, TGF-β, the best-defined profibrotic cytokine in HF mainly produced by cardiac myofibroblasts, is also up-regulated in the LV of WT mice but not TCR-$\alpha^{-/-}$ mice, but the source of TGF-β and the mechanisms involved in its release in the context of T cell–mediated inflammation are unclear. Thus, further investigation is warranted. In the present study, we hypothesized that IFN-γ–producing activated T cells (Th1 cells) perpetuate the fibrotic response in the setting of LV pressure overload through direct interaction with and regulation of CFB, leading to their differentiation into ECM-producing myofibroblasts. Here we report that nonantigen specific Th1 cells are sufficient to induce activation of CFB and release of TGF-β by CFB in vitro. We further demonstrate that T cell–CFB adhesion mediated by α4 integrin is required to acquire a profibrotic phenotype in vitro mediated by TGF-β. We also report that Th1 cells, but not activated IFN-$\gamma^{-/-}$ Th cells, can restore LV fibrosis and partially induce cardiac dysfunction in vivo in adoptively transferred TCR-$\alpha^{-/-}$ mice subjected to TAC.

RESULTS

T cells activated in response to pressure overload induced by TAC promote fibroblast transition to myofibroblast in vitro

We and others have previously shown that pressure overload induced by TAC results in T cell activation in the mLNs, and this correlates with T cell LV infiltration and the development of CF. Moreover, TCR-$\alpha^{-/-}$ and MHC-$II^{-/-}$ mice, deficient in $CD3^+$ T cells and $CD4^+$ T cells, respectively, do not develop CF or HF in response to TAC (Laroumanie et al., 2014; Nevers et al., 2015). We therefore sought to explore the role of T cells induced by TAC on CFB transition to profibrotic myofibroblasts initially using an in vitro approach. WT mice were subjected to 4 wk of TAC, a duration sufficient to induce CF and dysfunction, or sham surgery. The frequency of $CD4^+$ T cells was significantly increased in the mLNs of TAC but not of sham-operated mice (Fig. 1, A and B). In contrast, distal LNs such as the inguinal and mesenteric ones did not show such $CD4^+$ increase in response to TAC (Fig. 1, C and D), indicating that a $CD4^+$ T cell immune response is taking place specifically in the mLNs that drain the heart. Within the $CD4^+$ cells expanded in the mLN, we observed an increase in IFN-γ^+ cells in TAC mice as compared with sham (Fig. 1, E and F). IL-$17A^+CD4^+$ T cell and $Foxp3^+CD4^+$ T cell frequencies did not change between sham and TAC mice (Fig. S1). We next evaluated the effects of co-culturing $CD4^+$ T cells isolated from mLN of Sham or TAC mice with isolated CFB from WT mice. Co-culture of $CD4^+$ T cells purified from these groups with CFB revealed that $CD4^+$ T cells from TAC mice firmly adhered to CFB, in contrast with $CD4^+$ T cells isolated from sham-operated mice (Fig. 1, G and H). To evaluate the possibility that T cells were adhering to contaminating macrophages in the culture in addition to CFB, we performed staining with CD45, CD11b, and CD64 before (right after the heart digest and before the initial plating step of the CFB culture) and after CFBs were ready to be co-cultured with the T cells as indicated in the Materials and methods section. We found minimal contamination of $CD45^+CD11b^+CD64^+$ cells in the CFB preparation. Whereas the heart digest showed a mean of 26% of $CD45^+$ cells, and 35.8% of them coexpressing CD11b and CD64, the CFB preparation had <1% of $CD45^+$ cells. Within this minor $CD45^+$ cell population present in the CFB cultures, a mean of 70% coexpressed CD11b and CD64, but their frequency was minimal within the whole CFB preparation (Fig. 1 I). In addition, we found that CFB did not express F4/80, a marker of activated macrophages, in contrast to bone marrow–derived activated macrophages, which were used as a positive control (Fig. 1 J). The observed T cell adhesion to these CFB cultures negative for F4/80 and minimally expressing $CD45^+CD11b^+CD64$, quantified in several fields of view, induced the transition of CFB to myofibroblasts as demonstrated by increased expression of the contractile protein and myofibroblast marker α-SMA (Fig. 1, K and L). Thus, $CD4^+$ T cells activated in the mLNs and expressing mainly IFN-γ in the setting of

TAC-induced nonischemic HF adhere to CFB and induce CFB transition to profibrotic myofibroblasts.

Effector IFN-γ–producing Th1 cells promote α4 integrin–mediated contact-induced fibroblast transition to myofibroblasts in vitro

We have previously demonstrated that Tbet and IFN-γ, the signature transcription factor and cytokine of Th1 cells, were both elevated in the LV in response to TAC (Nevers et al., 2015). We confirmed this finding and additionally found that IL-4 and IL-5, the signature cytokines of Th2 cells, were not up-regulated in the LV in response to TAC, and their levels in the LV were significantly decreased as compared with IFN-γ (Fig. 2 A). Moreover, IFN-γ^+ $CD4^+$ cells were elevated in the mLNs in TAC mice compared with control sham mice (Fig. 1, E and F). Thus, we hypothesized that Th1 effector cells cross talk with CFB and promote the transition to myofibroblasts. We therefore next investigated whether Th1 cells were capable of inducing CFB-myofibroblast transition in co-culture experiments. We also co-cultured CFB with naive $CD4^+$ T cells, which lack the properly activated adhesion ligands required to infiltrate inflamed tissues and are not present in the heart (Germain, 1994; Alcaide et al., 2012; Burzyn et al., 2013). Additionally, CFBs were also cultured with IFN-$\gamma^{-/-}$ $CD4^+$ T cells (IFN-$\gamma^{-/-}$ Th cells), which were activated in vitro in the same Th1-polarizing conditions as WT cells but do not differentiate into IFN-γ–producing Th1 cells (Fig. S2). In contrast to naive $CD4^+$ T cells, effector Th1 cells added at a CFB/Th1 ratio of 5:1 (5 CFB per 1 Th1) firmly adhered to CFB and induced their transition to myofibroblasts expressing α-SMA (Fig. 2, B, C, and E). Interestingly, within the same co-culture, those CFBs with many adherent Th1 cells transitioned to α-SMA–expressing myofibroblasts, opposite to CFB supporting less or lack of Th1 adhesion, which expressed only basal levels of αSMA expression (Fig. 2, C–E). Moreover, when CFBs were co-cultured with increasing numbers of Th1 cells, regardless of the number of Th1 cells in the co-culture, those CFBs supporting Th1 cell adhesion became αSMA–expressing myofibroblasts (Fig. 2 F), and the higher number of T cells present in the co-culture correlated with a higher frequency of CFB supporting Th1 cell adhesion (96 ± 2% of CFB supporting Th1 cell adhesion at the CFB/Th ratio of 5:1 versus 22 ± 3.6% doing so at the CFB/Th1 1:5 ratio; Fig. 2, F and G). As expected, Th1 cell adhesion at the CFB/Th1 5:1 ratio was sufficient to mediate increased expression of α-SMA upon contact versus CFB alone expressing low but detectable levels of α-SMA. Of note, increased adhesion of Th1 cells to CFB (CFB/Th1 1:5 ratio resulting in over 90% of CFB supporting Th1 cell adhesion) resulted in a further increase in overall α-SMA in the co-culture compared with the CFB/Th1 5:1 ratio, a condition in which fewer CFBs support Th1 cell adhesion (Fig. 2 H). Thus, increased adhesion of Th1 with CFB results in increased CFB transformation. In contrast, CFB co-cultured with Th1 cells in transwells, and therefore exposed to Th1-released cytokines and soluble factors in the absence of direct contact, expressed significantly decreased levels of α-SMA compared with CFB that had been in direct contact with Th1 cells (Fig. 2, I and J). Moreover, IFN-$\gamma^{-/-}$ Th cells, which were activated as depicted by the expression of CD69 (Fig. 2 K) but cannot differentiate into IFN-γ–producing Th1 cells (Fig. S2), only slightly induced CFB transformation to α-SMA–expressing myofibroblasts in similar co-culture conditions (Fig. 2, L and M). Further studies evaluating T cell adhesion to CFB revealed that lower numbers of IFN-$\gamma^{-/-}$ Th cells adhered to CFB as compared with WT Th1 cells (Fig. 2, N and O). To confirm this was a Th1 cell–induced phenomenon in CFB and not in macrophages that are minimally present in the CFB preparations (Fig. 1, I and J), or that are not detected by CD45, CD11b, and CD64 costaining or by F4/80, we performed similar studies in clodronate liposomes–treated CFB preparations. Our results indicate that Th1 cells induced similar α-SMA expression upon adhesion to either clodronate-treated CFB (devoid of potential contaminating macrophages) or to untreated CFB (Fig. S3). Collectively, these data indicate that Th1 cells are responsible for CFB transformation to myofibroblasts upon direct contact, rather than by T cell cytokine release, and additionally demonstrate that T cell adhesion to CFB and induction of α-SMA expression upon adhesion are both dependent on IFN-γ.

We next investigated the specific T cell or CFB molecules adhesion molecules mediating this interaction. We focused on integrin–integrin ligand-mediated leukocyte adhesion. Function blocking antibodies to T cell α4 integrin resulted in impaired adhesion of Th1 cells to CFB compared with isotype control–treated Th1 cells. In contrast, intercellular adhesion molecule 1 (ICAM-1) deficiency in CFB had no effect in Th1 adhesion to CFB compared with WT CFB (Fig. 3, A and B). Moreover, blocking of α4 integrin resulted in decreased CFB expression of α-SMA, whereas lack of ICAM-1 in CFB had no effect on Th1-induced CFB expression of α-SMA (Fig. 3, C and D). Collectively, these data support that Th1 cells induce CFB transition to myofibroblasts through a mechanism that involves integrin α4–mediated adhesion.

Th1 adhesion induces TGF-β in cardiac fibroblasts and their transformation into profibrotic myofibroblasts

TGF-β is one of the most extensively studied profibrotic cytokines, and CFB are thought to be the predominant source of TGF-β in the heart. Numerous studies have demonstrated that inhibition of the TGF-β pathway attenuates fibrosis (Nakamura et al., 2000; Fukasawa et al., 2004; Teekakirikul et al., 2010). Thus, we tested the requirement of TGF-β for Th1 effector T cell adherence to CFB and induction of CFB-myofibroblast transition. We neutralized TGF-β in co-cultures of adult CFBs with naive T cells or Th1 cells. Anti–TGF-β antibody reduced TGF-β concentration in supernatants of CFB co-cultured with naive or Th1, as measured by ELISA (Fig. 4 A). As expected, naive T cells did not adhere to CFB in either control or anti–TGF-β conditions. However,

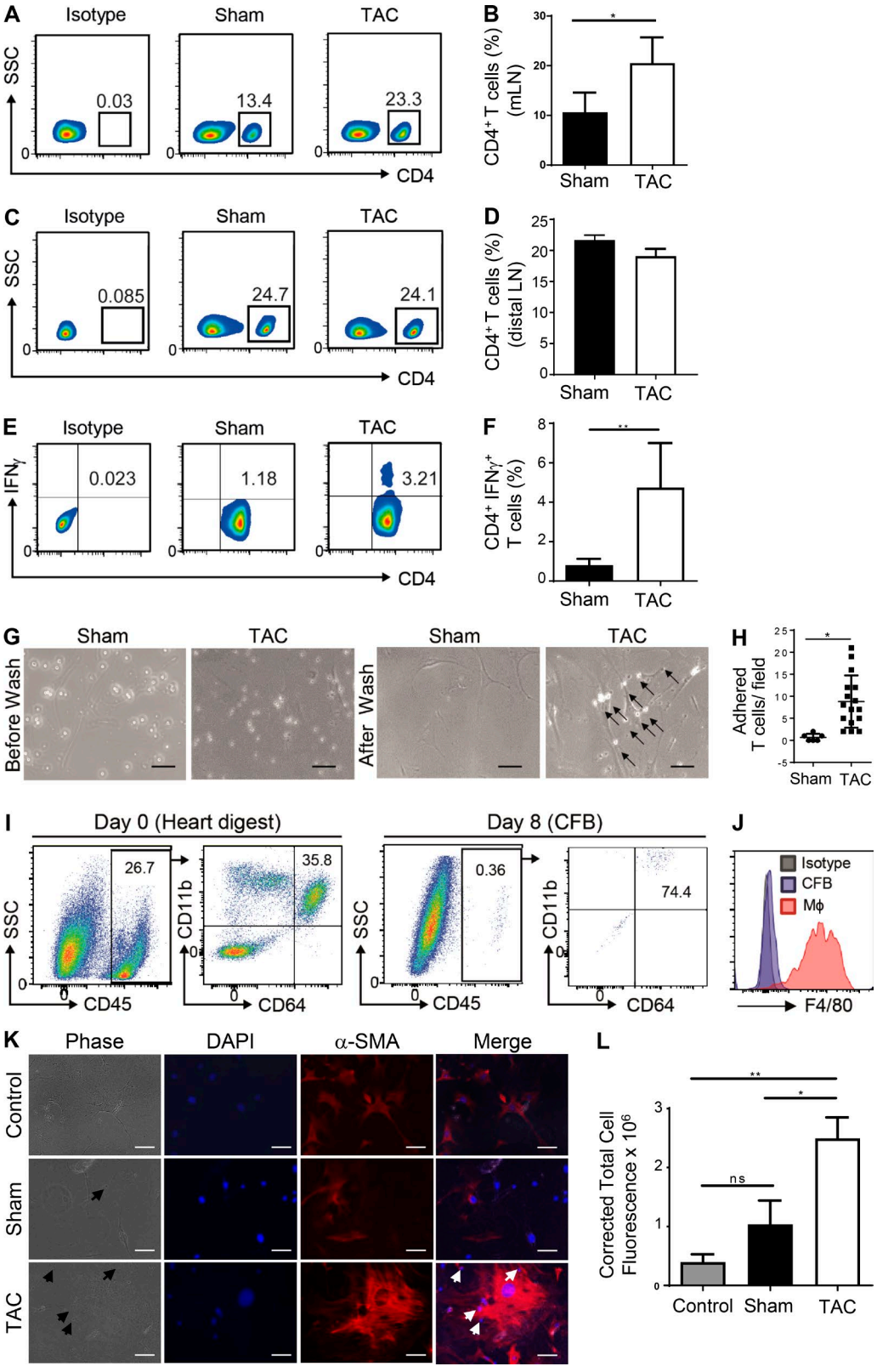

Figure 1. **T cells activated in response to TAC are mainly IFN-γ+, adhere to CFBs, and induce their transition to α-SMA expressing profibrotic myofibroblasts.** (A) Representative FACS plots and (B) quantification of the percentage of CD4 T cells in the mLNs and (C and D) in the inguinal and mesenteric LNs after 4 wk of sham or TAC surgery ($n = 5$ sham, $n = 8$ TAC, $P \leq 0.05$, Mann-Whitney test). (E) Representative FACS plots and (F) quantification of

compared with control antibody, TGF-β–neutralizing antibody did not reduce Th1 cell adhesion to CFB (Fig. 4, B and C). TGF-β–neutralizing antibody inhibited Th1-mediated induction of CFB-myofibroblast transformation as determined by α-SMA expression (Fig. 4, D and E). To evaluate the source of TGF-β upon Th1-CFB adhesion, we performed studies in which adherent Th1 cells were detached from the CFB with EDTA to disrupt integrin α4 calcium–dependent interactions, and evaluated TGF-β expression by flow cytometry. Likewise, CFB detached from Th1 cells, and co-cultured Th1 cells that did not bind to CFB were similarly evaluated for TGF-β expression. We found that neither Th1 cells that did not adhere to the CFB (washed after the co-culture with media) nor Th1 cells adherent to CFB but detached with EDTA expressed TGF-β. On the other hand, the population of CFB washed of adherent Th1 cells by EDTA expressed TGF-β as determined by flow cytometry (Fig. 4 F). Moreover, immunofluorescence staining demonstrated that CFB expressed TGF-β after co-culture with Th1 cells, but not with naive T cells (Fig. 4 G). Collectively, these data support that TGF-β does not mediate adhesion of Th1 cells to CFB, and demonstrate that TGF-β produced by CFB upon Th1 cell adhesion is responsible for Th1 contact induced CFB transformation to myofibroblasts.

Adoptive transfer of IFN-γ–producing Th1 effector T cells into recipient TCR-$\alpha^{-/-}$ mice induces LV inflammation, perivascular CF, and LV TGF-β up-regulation

We and others previously demonstrated that T cell–deficient mice do not develop CF in response to TAC, implying a role for T cells in the development of CF (Laroumanie et al., 2014; Nevers et al., 2015). Because our in vitro data demonstrated that Th1 cells induce the transition of CF to myofibroblasts, we next tested whether Th1 cells induced CF in vivo. TCR-$\alpha^{-/-}$ mice were reconstituted with naive control T cells, Th1 cells generated in vitro from WT mice, or IFN-$\gamma^{-/-}$–activated Th cells. TCR-$\alpha^{-/-}$ mice received TAC or sham control surgery, followed by adoptive transfer (AT) of 10 million naive $CD4^+$ T cells, Th1 effector T cells, or IFN-$\gamma^{-/-}$ Th cells at 48 h and again at 2 wk after surgery (Fig. 5 A). TCR-$\alpha^{-/-}$ mice undergoing TAC or sham surgery without T cell reconstitution were used as controls (no AT). T cell frequency after AT was measured by flow cytometry in distal LNs and spleen, and showed a significant increase of peripheral T cells compared with TCR-$\alpha^{-/-}$ control mice that did not receive any T cells (Fig. 5, B–E). Specifically, reconstitution of TAC TCR-$\alpha^{-/-}$ mice with Th1 cells or with IFN-$\gamma^{-/-}$ Th cells resulted in a mean of 24.9 ± 1.3% versus the basal 1.26 ± 0.3% of $CD4^+$ T cells found in TCR-$\alpha^{-/-}$ control mice (Mombaerts et al., 1992; Burzyn et al., 2013). Naive $CD4^+$ T cell reconstitution resulted in 5.73 ± 0.8%, significantly less than activated Th1 and activated IFN-$\gamma^{-/-}$ Th cells, likely because of lack of activation in the host.

In contrast to naive T cells, AT of Th1 effector cells after TAC led to a significant increase in $CD4^+$ T cell infiltration into the LV, predominantly in perivascular areas. Activated IFN-$\gamma^{-/-}$ Th cells were able to infiltrate the LV but in significantly smaller numbers than Th1 cells (Fig. 5, F and G). Transfer of Th1 effector T cells, but not naive or IFN-$\gamma^{-/-}$ Th cells, also increased LV expression of the Th1 signature transcription factor Tbet compared with TCR-$\alpha^{-/-}$ TAC mice not receiving any T cells (Fig. 5 H), indicating the likely presence of $Tbet^+$ Th1 cells. Thus, AT of Th1 and IFN-$\gamma^{-/-}$ Th cells into TCR-$\alpha^{-/-}$ mice successfully reconstituted $CD4^+$ T cells in lymphoid tissue, but Th1 cells infiltrated the LV in response to TAC in higher numbers than naive or IFN-$\gamma^{-/-}$ Th cells. AT of Th1 effector T cells also significantly increased the LV expression of proinflammatory cytokines IL-6 and IL-1β compared with TAC TCR-$\alpha^{-/-}$ that were not reconstituted with T cells. In contrast, AT of naive or activated IFN-$\gamma^{-/-}$ Th cells did not result in such increase (Fig. 5, I and J). Moreover, only AT of TCR-$\alpha^{-/-}$ mice with Th1 cells, but not with naive or activated IFN-$\gamma^{-/-}$ Th cells, induced perivascular fibrosis as depicted by the observed collagen deposition in perivascular areas in LV sections (Fig. 6, A and B). Strikingly, transfer of Th1 cells did not restore interstitial fibrosis in TCR-$\alpha^{-/-}$ mice (Fig. 6, A and C), in contrast with WT mice that develop both interstitial and perivascular fibrosis, as we and others have previously described (Xia et al., 2009; Nevers et al., 2015). Systemically, Th1 cells, but not naive T cells, induced an increase in serum circulating levels of TGF-β in TCR-$\alpha^{-/-}$ mice, to levels comparable with those observed in WT TAC mice (Fig. 6 D). Immunofluorescence of LV tissue demonstrated that TGF-β expression was increased in the LV at the areas that colocalized with augmented perivascular fibrosis in TCR-$\alpha^{-/-}$ mice transferred with Th1 cells but not with naive cells (Fig. 6 E). Collectively, these data demonstrate a critical profibrotic and proinflammatory role for IFN-γ produced by Th1 cells and support that T cell activation in the absence of IFN-γ is not sufficient to induce LV inflammation and fibrosis in vivo.

the percentage of $CD4^+IFN\text{-}\gamma^+$ T cells in the mLNs after 4 wk of sham or TAC surgery. One representative FACS plot is shown from $n = 5$–8 mice per group ($P \leq 0.05$, Mann-Whitney test). (G) Representative photo micrographs of $CD4^+$ T cells purified from mLN of 4-wk sham or TAC mice adhering to CFB after overnight co-culture. Cells were co-cultured at a 5:1 ratio (CFB/T cells) and pictures were taken before and after washing the culture with media (arrows indicate T cells that remained adhered to CFB). (H) Quantification of $CD4^+$ T cells that adhered to CFB after washing in three to five separate fields of view ($n = 3$ separate experiments; $P \leq 0.05$, Student *t*-test). (I and J) Representative FACS with the indicated Abs at the initial and final step of the CFB preparations. $n = 3$ independent CFB preparations. Activated bone marrow isolated macrophages (Mφ, in red) are used as a positive control in J. Numbers in all FACS plots represent percentage. (K and L) Immunofluorescence staining (K) and quantification of α-SMA expression (L) on resting CFB (control) or CFB after overnight co-culture with $CD4^+$ T cells from sham or TAC mice (arrows indicate T cells adhering to CFB). Bars, 50 µm. Error bars represent mean ± SD. *, $P < 0.05$; **, $P = 0.01$; ns, not significant; one-way ANOVA test; $n = 3$ independent experiments.

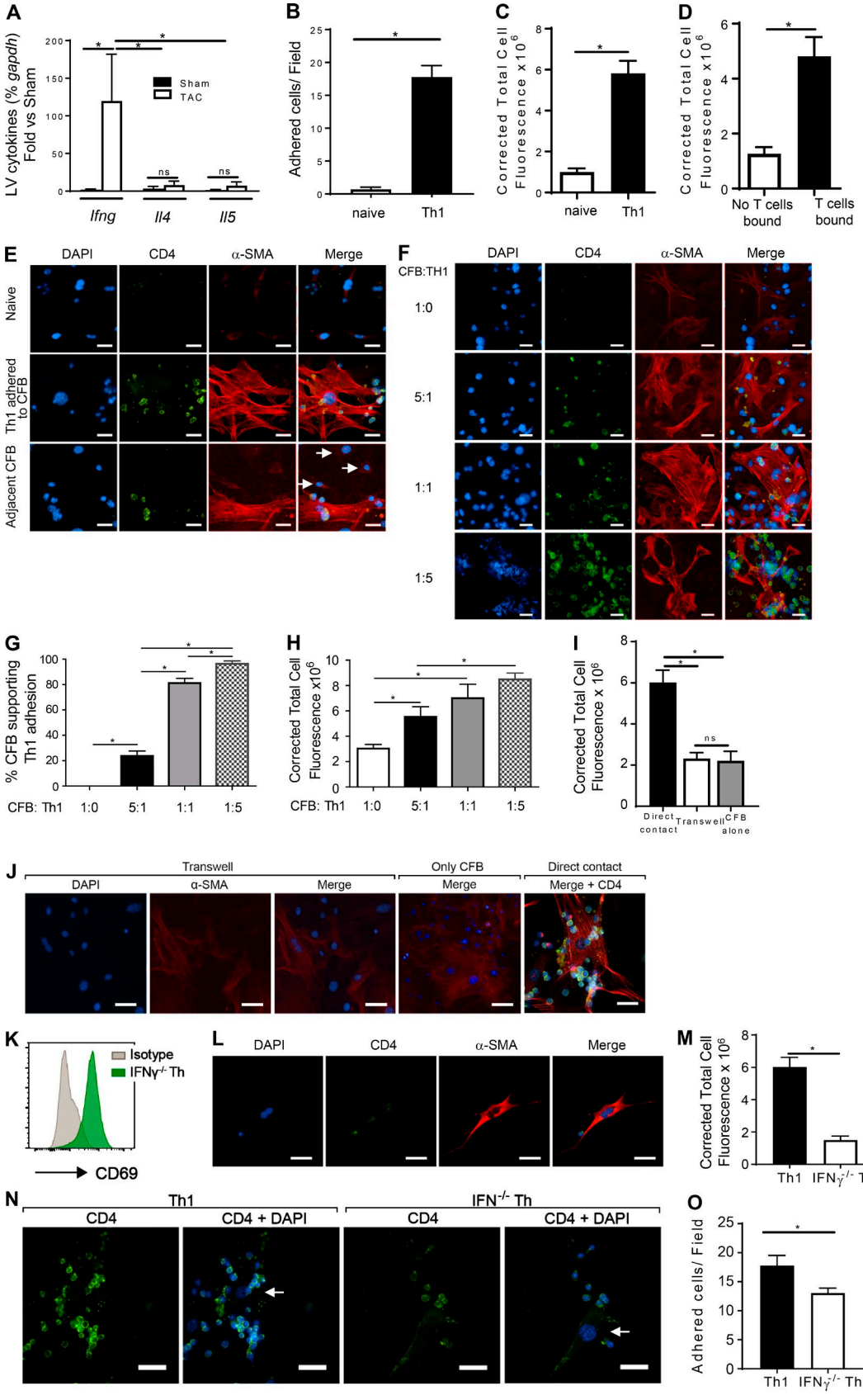

AT of Th1 cells partially reverses the LV functional protection of TCR-$\alpha^{-/-}$ mice subjected to the TAC model of HF

We next examined cardiac function through echocardiography and invasive LV hemodynamic studies in TCR-$\alpha^{-/-}$ mice subjected to sham or TAC surgery that had been reconstituted with either no cells (no AT), naive T cells, Th1 effector cells, or IFN-$\gamma^{-/-}$ Th cells, as described in Fig. 5 A. We further evaluated WT sham and TAC mice as a positive control of TAC-induced LV dysfunction. TAC induced a similar degree of pressure overload in all groups studied, as measured by peak LV systolic pressure (Fig. 7 A). Similar to what we had previously described, TAC resulted in increased LV weight in WT mice but not in TCR-$\alpha^{-/-}$ compared with sham controls (Nevers et al., 2015). AT of naive, Th1, or IFN-$\gamma^{-/-}$ Th cells into TCR-$\alpha^{-/-}$ TAC mice resulted in increased LV weight compared with TAC TCR-$\alpha^{-/-}$ not receiving any T cells (Fig. 7 B) and LV cardiomyocyte size determined in LV cross sections was also increased to the level of WT TAC in all TCR-$\alpha^{-/-}$ TAC mice receiving T cells (Fig. 7 C). Additionally, as previously reported, TAC induced increased wall thickness in WT mice but not in TCR-$\alpha^{-/-}$ compared with their respective sham groups. However, only AT of Th1 T cells in TCR-$\alpha^{-/-}$ TAC mice specifically resulted in increased wall thickness that was statistically significant compared with TCR-$\alpha^{-/-}$ TAC not receiving any T cells. In contrast, AT of naive or IFN-$\gamma^{-/-}$ Th cells only showed a trend to increased wall thickness as compared with TCR-$\alpha^{-/-}$ TAC mice (Table 1). LV chamber dimensions determined by echocardiography (end diastolic and end systolic diameter), on the other hand, remained unchanged upon AT of Th1 cells (Table 1). Further analysis of LV hemodynamics revealed selective effects of adoptively transferred Th1 effector T cells, but not naive or activated IFN-$\gamma^{-/-}$ Th cells, on LV function in the TCR-$\alpha^{-/-}$ TAC mice. LV end diastolic pressure (LVEDP) increased in WT TAC mice compared with WT sham as expected, indicating the development of HF. TCR-$\alpha^{-/-}$ TAC mice did not develop elevated LVEDP, consistent with our prior published results (Nevers et al., 2015). Interestingly, AT of Th1 cells, but not naive T cells or IFN-$\gamma^{-/-}$ Th cells, resulted in increased LVEDP in TCR-$\alpha^{-/-}$ TAC mice to values higher than those in TCR-$\alpha^{-/-}$ TAC mice not receiving any T cells, but lower in magnitude than those achieved by WT mice (Fig. 7 C). LV contractile function determined by the peak rate of LV pressure rise (dp/dt_{Max}) was likewise significantly improved in TCR-$\alpha^{-/-}$ TAC mice compared with WT TAC, as reported previously (Nevers et al., 2015), whereas reconstitution of TCR-$\alpha^{-/-}$ TAC mice with Th1 cells resulted in reduced dp/dt_{Max} compared with TCR-$\alpha^{-/-}$ TAC mice that either did not receive any T cells or were adoptively transferred with naive or with IFN-$\gamma^{-/-}$ Th cells (Fig. 7 D). Furthermore, Th1 cells but not naive T cells or activated IFN-$\gamma^{-/-}$ Th cells induced an increased ratio of β- over α-myosin heavy chain isoforms in the LV of TCR-$\alpha^{-/-}$ TAC mice, indicating fetal gene reexpression, a marker of pathological cardiac myocyte hypertrophy and remodeling, but not to the extent of the increase observed in WT mice (Fig. 7 E). In particular, the fetal isoform of myosin heavy chain (MHC), MHC-β, was the most significantly increased in WT TAC mice (20-fold induction vs. WT sham) and in TCR-$\alpha^{-/-}$ TAC mice that received Th1 cells (3.8-fold induction vs. TCR-$\alpha^{-/-}$ sham) and remained unchanged in TCR-$\alpha^{-/-}$ TAC mice receiving naive or IFN-$\gamma^{-/-}$ Th cells. MHC-α was not altered in WT TAC versus WT sham, and also remained unchanged in TCR-$\alpha^{-/-}$ TAC mice AT with the different T cell types. The expression of other genes associated with cardiac hypertrophy, but not with cardiac dysfunction, such as atrial natriuretic peptide (ANP) and brain natriuretic peptide (BNP), were increased in mice AT with both Th1 cells and IFN-$\gamma^{-/-}$ Th cells but not to the same extent as in WT TAC mice (Fig. S4). Collectively, these data demonstrate that although all T cell subsets evaluated induce LV hypertrophy, only IFN-γ–producing Th1 cells contribute to pathological LV functional decrement as revealed by LVEDP, dp/dt_{Max}, and fetal gene reexpression of MHC-β.

Figure 2. **Th1 cell adhesion to CFB induces CFB transition to α-SMA expressing profibrotic myofibroblasts.** (A) qRT-PCR of IFN-γ, IL-4, and IL-5 in the LV of WT mice subjected to TAC or sham surgery (n = 5 sham, n = 8 TAC; $P \leq 0.05$; one-way ANOVA test). (B) Quantification of naive and Th1 cell adhesion to CFB and of (C) α-SMA expression in overnight co-cultures of CFB with naive or effector Th1 cells polarized in vitro. Numbers represent T cells that remained bound in three to five separate fields of view after washing the co-culture (n = 5 independent experiments; $P \leq 0.05$, Student t-test). (D) Quantification and (E) representative photo micrographs indicating adhesion of $CD4^+$–Alexa Fluor 488–labeled T cells to CFB after overnight co-culture and washing. Pictures represent immunofluorescence staining of areas of CFB supporting Th1 cell adhesion (Th1 adhered to CFB) versus adjacent CFB not supporting Th1 adhesion (adjacent CFB indicated with white arrows) next to CFB supporting Th1 adhesion. Quantification represents three to five separate fields of view in n = 5 independent experiments, $P \leq 0.05$ Student t-test. (F) Representative photo micrographs indicating adhesion of the indicated CFB: $CD4^+$–Alexa Fluor 488–labeled Th1 ratios after overnight co-culture and washing (only CFB supporting Th1 adhesion are shown) and (G) quantification of CFB supporting Th1 adhesion and (H) α-SMA expression in the different co-culture conditions (including all CFB supporting and not supporting Th1 adhesion). Analysis performed in n = 3–5 fields of view per condition; n = 2 independent experiments; $P \leq 0.05$, Student t-test. (I) Quantification and (J) representative immunofluorescence photo micrographs of α-SMA staining after overnight co-culture of CFB with Th1 cells (5:1) in Transwells to avoid direct contact. Analysis performed in n = 3–5 fields of view; n = 3 independent experiments; $P \leq 0.05$, one-way ANOVA test. (K) Representative FACS histogram of activated IFN-$\gamma^{-/-}$ Th cell. (L) Representative micrographs of co-cultured CFB with activated IFN-$\gamma^{-/-}$ Th cell and (M) quantification of α-SMA expression upon overnight co-culture. (N) Representative pictures of Th1 and IFN-$\gamma^{-/-}$ Th cells (green) adhered to CFB (white arrows) and (O) quantification of T cell adhesion to CFB. Analysis performed in n = 3–5 fields of view; n = 3 independent experiments; $P \leq 0.05$, Student t-test. Bars, 50 µm. Error bars represent mean ± SD. *, $P < 0.05$. ns, not significant.

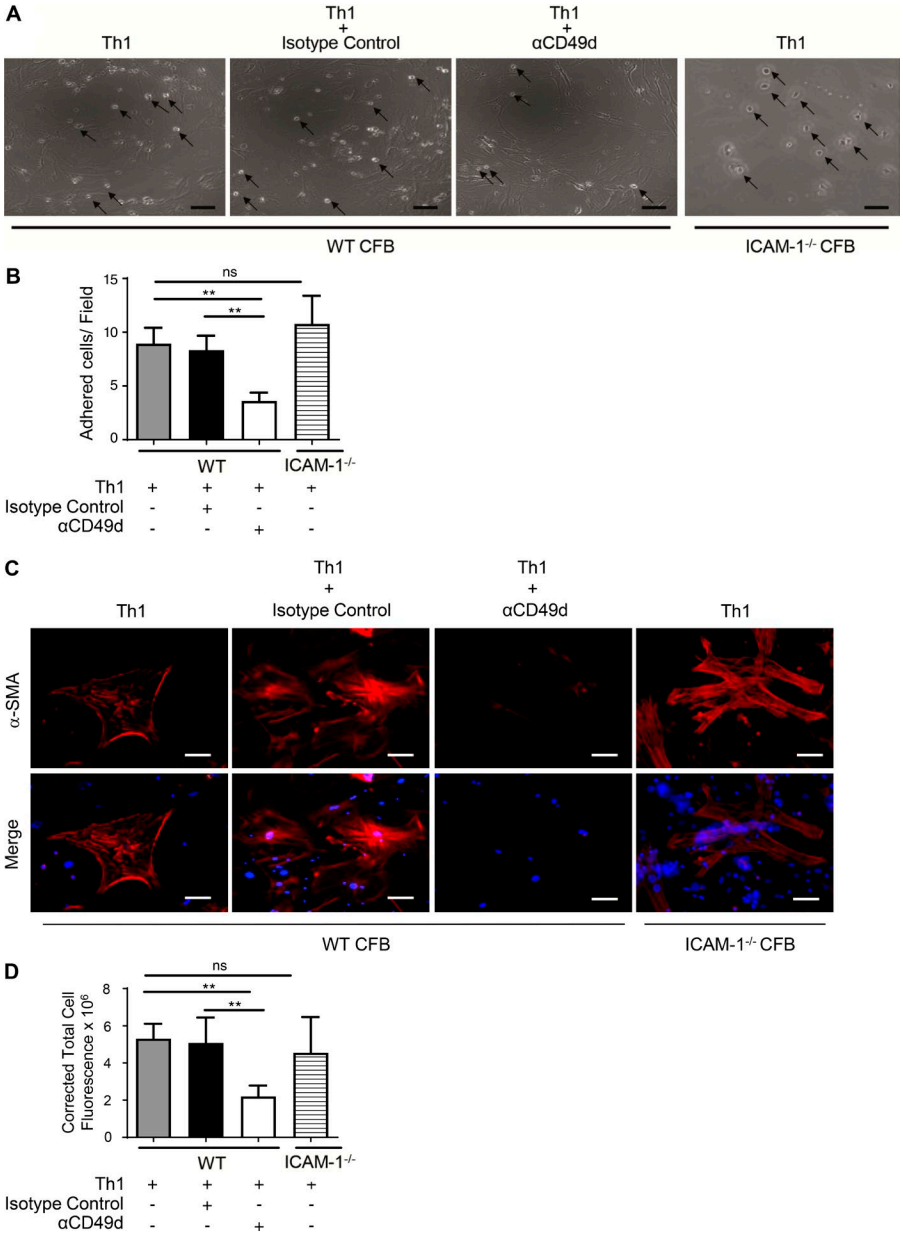

Figure 3. **Th1 cells adhere to CFB through α4 integrin.** (A and B) Representative photo micrograph (A) and quantification (B) of Th1 cells adhesion to either WT CFB or ICAM-1$^{-/-}$ CFB after overnight co-culture. α4 integrin was blocked with αCD49d antibody on Th1 T cells or isotype control before culturing with WT CFB overnight at a 5:1 ratio (CFB/T cells). Isotype-matched antibody was used as a control. Arrows point to T cells adhering to indicated WT or ICAM-1$^{-/-}$ CFB. Analysis performed in n = 3–5 fields of view; n = 3 independent experiments; P ≤ 0.05, one-way ANOVA test. (C) Immunofluorescence staining of α-SMA expression after overnight co-culture of adult WT CFB with Th1 cells, or Th1 cells treated with α4 integrin blocking antibodies (αCD49d) or isotype control, or Th1 cells co-cultured with adult ICAM-1$^{-/-}$ CFB. (D) Quantification of α-SMA corrected total cell fluorescence in n = 3–5 fields of view; n = 3 independent experiments; P ≤ 0.05, one-way ANOVA test. Bars, 50 µm. Error bars represent mean ± SD. **, P < 0.01. ns, not significant.

DISCUSSION

Despite significant advancements in medical therapies for HF, the prognosis of patients remains poor, with >50% mortality within 5 yr after the first hospital admission, regardless of whether the etiology is of ischemic or not ischemic origin (Mozaffarian et al., 2016). We and others have recently identified a critical role for T cells in promoting pathological cardiac remodeling in both ischemic and nonischemic HF (Wei, 2011; Hofmann et al., 2012; Laroumanie et al., 2014; Nevers et al., 2015; Salvador et al., 2016). In this study we investigated the CF mechanisms regulated by CD4$^+$ T cells and identified the effector IFN-γ–producing Th1 cell subset as a critical driver of CF and contributor to cardiac dysfunction using a well-established mouse model of nonischemic HF. We report that Th1 cell adhesion to CFB through α4 integrin is required to induce a profibrotic response that is dependent on TGF-β induction in CFB in vitro. In vivo, CF is primarily localized to the perivascular areas where Th1 cells selectively infiltrate the LV in TCR-α$^{-/-}$ recipient mice in response to TAC. Only Th1 cells, but not naive T cells or similarly activated IFN-γ$^{-/-}$ Th cells, partially restore CF, cardiac inflammation, fetal gene reexpression, and cardiac dysfunction.

Multiple studies over recent years have identified various innate immune cells actively participating in profibrotic tissue repair and healing in various tissues (Wilson and Wynn, 2009; Costa et al., 2011; Murray et al., 2011; Takemasa et al., 2012; Walsh et al., 2015) including the heart in response to ischemic myocardial injury (Frangogiannis et al., 2002; Fran-

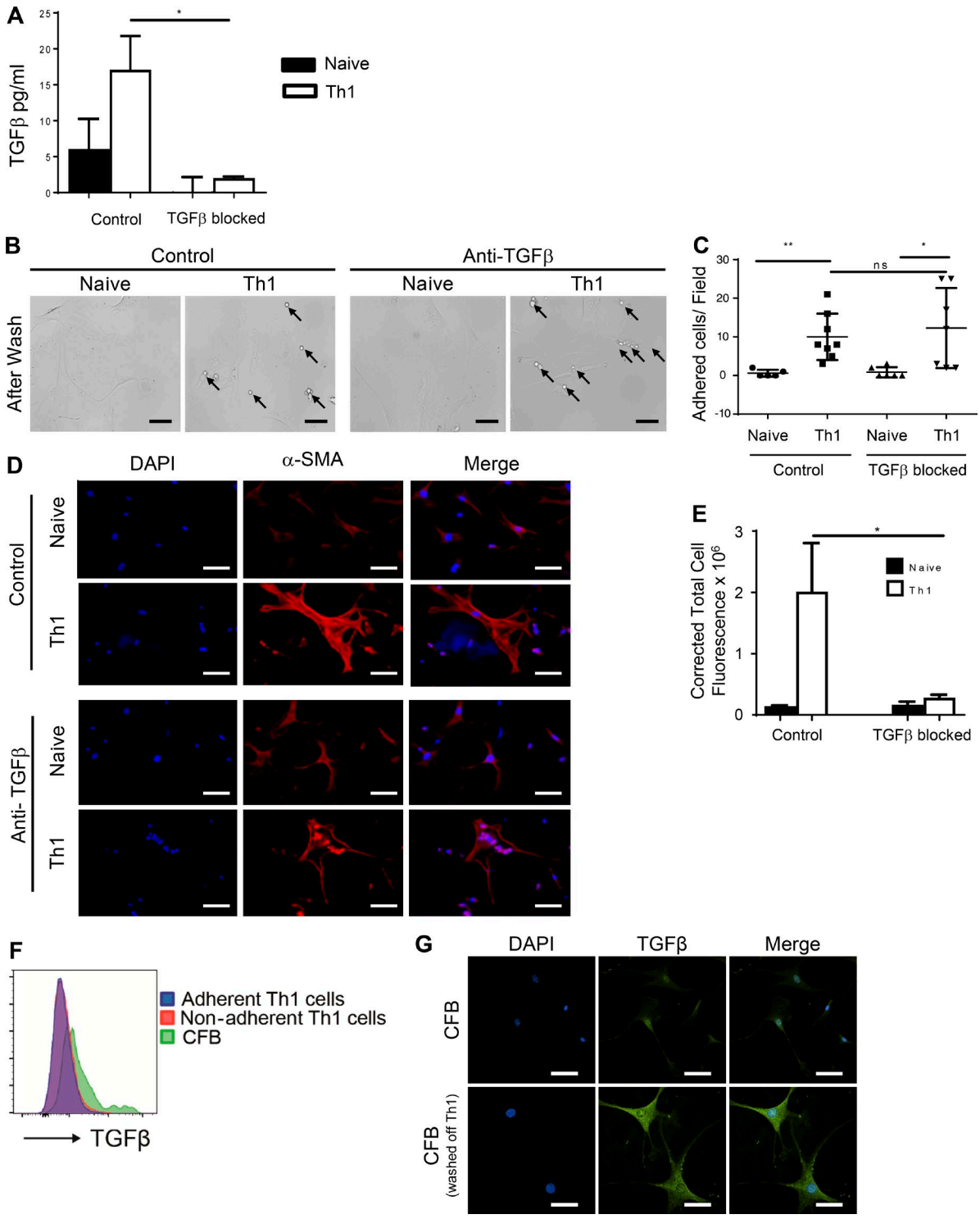

Figure 4. **Th1 adhesion to CFB induces TGF-β in CFB and their transition to α-SMA expressing profibrotic myofibroblasts.** Neutralization of TGF-β in CFB/T cell co-culture inhibits CF transition to α-SMA expressing profibrotic myofibroblasts. (A) Quantification of TGF-β in supernatants of the indicated co-cultures with or without TGF-β neutralization antibody (n = 3 independent experiments; $P \leq 0.05$, one-way ANOVA test). (B) Representative photo micrographs of naive and effector Th1 cells adhering to adult CFB after overnight co-culture in the presence of TGF-β neutralization antibody or control untreated cells. Arrows indicate T cells that adhered to CFB. (C) Quantification of naive and Th1 $CD4^+$ T cells that adhered to cardiac fibroblast with (control) or without TGF-β neutralization. Numbers represent the number of T cells bound in n = 3–5 fields of view; n = 3 independent experiments; $P \leq 0.05$, one-way ANOVA test. (D) Immunofluorescence staining of α-SMA expression after overnight co-culture with control unstimulated CFB, naive, or Th1 cells treated with TGF-β neutralization antibody or no antibody control. Bars, 50 µm. (E) Quantification of α-SMA expression in n = 3–5 fields of view; n =

gogiannis, 2004). Less was known about adaptive immunity until recently, when T cells were identified as critical mediators of profibrotic tissue repair and healing of the ischemic myocardium through mechanisms involving modulation of monocytes and macrophages differentiation that actively participate in profibrotic scar formation (Hofmann et al., 2012). In contrast to a profibrotic cardiac healing response, in nonischemic HF when the LV senses substantial pressure load, CF is mainly mediated by CFB, a major resident population in the heart, and is a pathological progressive process that impairs cardiac function (Fan et al., 2012). Interestingly, the role of T cells in this response is an emerging area with several unknowns. From our own and other investigators' earlier studies, we learned that T cells are central players in CF: in humans, we found an association between CF and cardiac T cell infiltration in patients with nonischemic HF (Nevers et al., 2015); and in mice, we and others demonstrated T cell activation in the mLNs in response to TAC, and found that two different mouse models lacking either αβ T cells (TCR-$\alpha^{-/-}$ mice) or $CD4^+$ T cells (MHC-$II^{-/-}$ mice) were protected from CF induced by TAC (Laroumanie et al., 2014; Nevers et al., 2015). This motivated us to consider that $CD4^+$ T cells activated in the setting of TAC could have direct effects in the CFB and induce their transformation to profibrotic myofibroblast. Our results provide for the first time evidence that T cells activated in the context of HF firmly adhere to CFB and, as a result, induce their transformation to profibrotic myofibroblasts. In contrast, T cells from sham mice, which are mostly naive, do not adhere and activate CFB. Our work indicates that IFN-γ, the signature cytokine of Th1 cells, is the main cytokine expressed by mLN $CD4^+$ T cells as well as in the LV in response to TAC. Other cytokines such as IL-5 and IL-4, known to mediate the profibrotic effect of Th2 cells (Sandler et al., 2003), are, in contrast, not enhanced after TAC in the LV, and IL-17A, also known to be profibrotic in autoimmune-induced dilated cardiomyopathy (Wu et al., 2014), was not detected in either the mLNs or the LV. Of note, Th2 and Th17 have recently been reported to be predominant in the failing hearts in mice with chronic ischemic HF (8 wk after ischemia) and found to be mainly expanded in the spleen (Bansal et al., 2017). Our data position IFN-γ–producing Th1 cells expanded in the mLNs as major contributors to TAC-induced CF, and highlight important differences about the type and location of T cell–mediated remodeling responses in ischemic versus nonischemic HF. Our results are in agreement with our previous work demonstrating that the Th1 signature transcription factor Tbet is significantly up-regulated in the LV in response to TAC in WT mice but not in TCR-$\alpha^{-/-}$ mice (Nevers et al., 2015). However, the contribution of Th1 cytokines, and in particular IFN-γ, to fibrosis is controversial, with some studies demonstrating an antifibrotic effect in the context of autoimmune-induced CF (Afanasyeva et al., 2004; Fairweather et al., 2004; Borthwick et al., 2013), and others a profibrotic effect in the context of hypertension and in healing after ischemia (Bujak et al., 2009; Han et al., 2012; Markó et al., 2012). Our in vitro results demonstrate a novel mechanism that positions IFN-γ–producing Th1 cells as profibrotic players in CF by directly adhering to the CFB rather than exclusively through Th1 cell cytokine release. This is further supported in our Th1 titration co-culture studies, in which more Th1 cell adhesion to CFB correlates with increased overall α-SMA expression in the co-cultures, whereas those CFBs supporting Th1 cell adhesion regardless of the CFB/Th1 ratio all express high levels of α-SMA.

Although our in vitro studies demonstrate that Th1 cytokine release does not induce CFB transformation, extending this observation in vivo will require further investigation. Whereas the profibrotic role of TGF-β in CF has been recognized for many years (Border and Noble, 1994; Bujak and Frangogiannis, 2007), the fact that Th1 cell adhesion induces TGF-β in the CFB is novel, and supports that IFN-γ–producing Th1 cells critically control CFB fate in vitro through direct cell–cell adhesion. Our data demonstrating that the few IFN-$\gamma^{-/-}$ Th cells that were able to adhere to CFB did not induce their transformation as WT Th1 cells did also support that T cell–produced IFN-γ centrally regulates CFB transformation to profibrotic myofibroblasts.

Cross talk between other T cell subsets, such as $CD4^+$ regulatory cells (Treg), and CFB has been previously reported in co-culture experiments in which Tregs were found to inhibit CFB transition to profibrotic myofibroblasts. The in vivo relevance of this finding was that Treg inhibited pathological postischemic cardiac remodeling acting on CFB in chronic ischemic HF (Saxena et al., 2014). This is in line with an antiinflammatory and antifibrotic role for Treg (Kanellakis et al., 2011), opposite from the proinflammatory and profibrotic role we describe for Th1 cells here. Whether Treg direct contact with the CFB or the antifibrotic effect observed involved TGF-β signaling in the CFB was not addressed in the co-culture or the in vivo studies. Our studies demonstrate that Tregs remain unchanged in the mLNs after TAC, and we previously reported that Foxp3 expression is significantly reduced in the LV compared with Tbet (Nevers et al., 2015). Here we also demonstrate that Th1 cells do not transform into TGF-β–producing T cells upon adhesion to CFB, in line with the literature supporting a lack of plasticity of

3 independent experiments; $P \leq 0.05$, one-way ANOVA test. (F) Nonadherent Th1 cells were collected from the Th1-CFB co-culture, adherent Th1 cells were detached from CFB with EDTA, and CFB detached of Th1 cells were tripsinized and collected for FACS staining. (G) Immunofluorescence staining of TGF-β in CFB alone and CFBs that had supported Th1 adhesion and were detached of Th1 cells. Bars, 50 µm. One representative FACS histogram and representative pictures from one representative immunofluorescence experiment are shown of a total of three independent experiments performed. Bars, 50 µm. Error bars represent mean ± SD. *, $P < 0.05$; **, $P < 0.01$. ns, not significant.

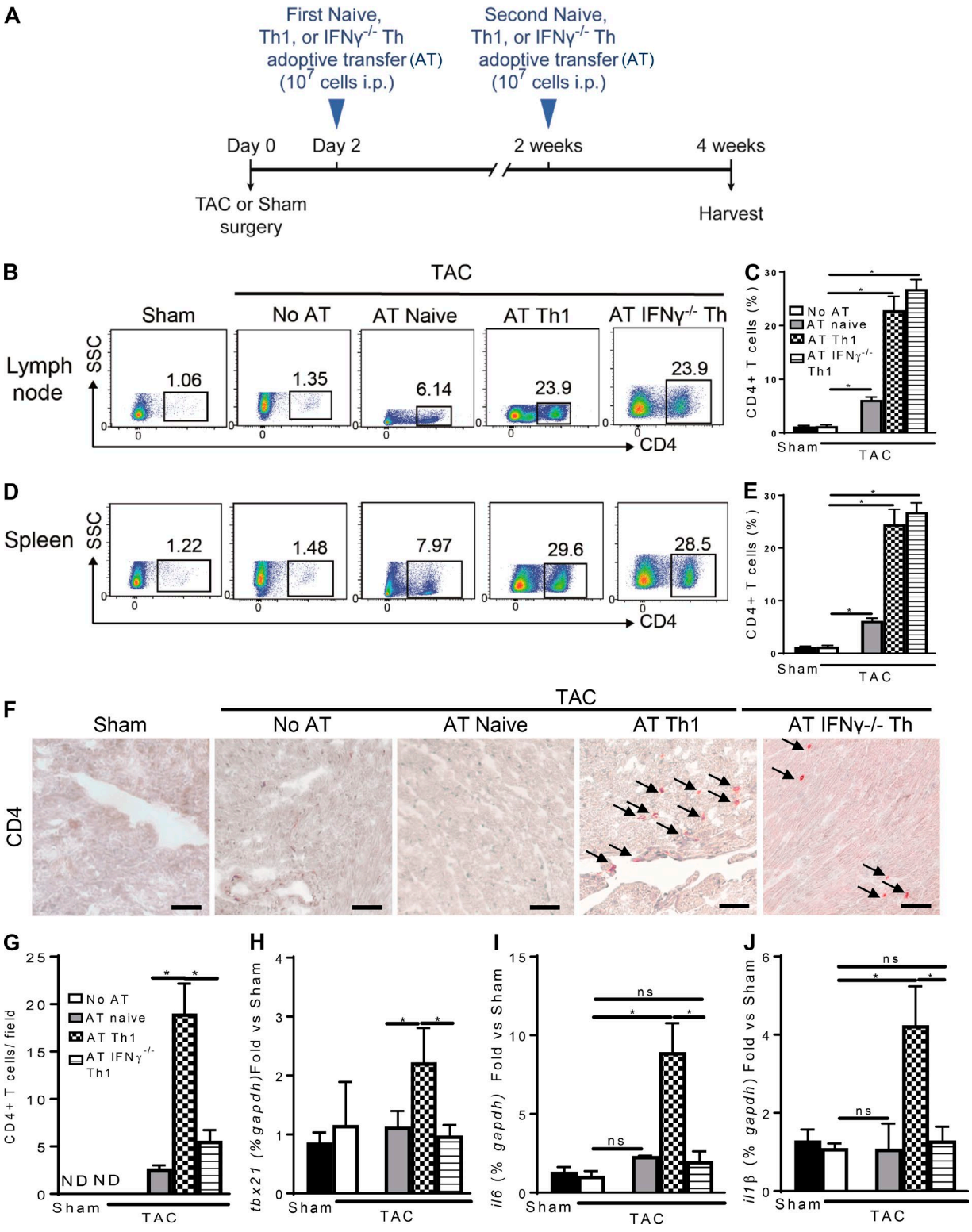

Figure 5. **TCR-$\alpha^{-/-}$ mice are successfully reconstituted with naive, Th1, and activated IFN-$\gamma^{-/-}$ Th cells, but only Th1 cells induce LV inflammation.** (A) Schematic representation of in vivo AT experiments. Forty-eight hours and 2 wk after TAC or sham surgery, 10^7 naive, Th1 cells, or IFN-$\gamma^{-/-}$ Th cells were adoptively transferred into TCR-$\alpha^{-/-}$ recipient mice, and tissues were harvested at 4 wk after TAC or sham surgery. (B–D) Representative FACS plots (B and D) and quantification (C and E) of peripheral $CD4^+$ T cells in the LNs (B and C) and the spleen (D and E) of control (no AT, TCR-$\alpha^{-/-}$ mice) or TCR-$\alpha^{-/-}$ mice reconstituted with the indicated T cells. Dot plots are representative of two to three independent AT experiments for each T cell subset transferred (n = 6–8

Th1 cells (Hirahara and Nakayama, 2016), although this had never been evaluated in the context of CFB adhesion. These results further support that the inhibitor effect of anti–TGF-β we observe is likely targeting TGF-β released by the CFB. A limitation of this study and something that will need to be evaluated in the future is the source of TGF-β and whether it is induced upon T cell contact in a more complex scenario in vivo, in which Th1 cells may also establish direct interactions with heart macrophages and/or endothelial cells and trigger similar or additional profibrotic mechanisms (Zeisberg et al., 2007; Chen and Frangogiannis, 2016).

One striking finding from our in vivo AT studies is that effector Th1 cells sufficiently convert the antifibrotic phenotype of TCR-$\alpha^{-/-}$ mice in response to TAC into a profibrotic phenotype. More striking is the fact that adoptively transferred Th1 cells, but not equally activated IFN-$\gamma^{-/-}$ Th cells, infiltrate mainly in perivascular areas of the LV, and induce perivascular but not interstitial fibrosis, in contrast to the predominantly interstitial pattern of T cell infiltration and both perivascular and interstitial fibrosis observed after TAC in WT mice (Nevers et al., 2015). We suggest that interstitial fibrosis, classically thought to originate from areas surrounding the microvasculature and spreading throughout the myocardium (Anderson et al., 1979; Weber, 1989), depends on the location of the infiltrated T cells and direct cross talk with the CFB. Importantly, the AT of Th1 cells on the TCR-$\alpha^{-/-}$ mice, normally protected from cardiac dysfunction, selectively impacted LV contractile function, but not diastolic function or LV chamber dimensions. Although the current paradigm holds that interstitial fibrosis is the main contributor to mechanical stiffness and cardiac dysfunction in HF (Chaturvedi et al., 2010), some studies have also suggested that perivascular fibrosis most likely induced by perivascular inflammation decreases the supply of oxygen and nutrients to the myocardium and can induce cardiac pathology (Kai et al., 2006). Our data suggest the possibility that Th1 cells infiltrating into perivascular areas could reduce coronary flow through reduction of intracoronary vessel diameters, or, by directing fibrosis, impairing diffusion of oxygen and nutrients to the myocardium. These vascular abnormalities could potentially account for the reduction in LV systolic function and resultant increase in end diastolic pressure. Cytokines such as IL-17A can alter vascular function this way (Nguyen et al., 2013), and although our results indicate that IL-17A is not significantly increased in response to TAC, IFN-γ released by Th1 cells could potentially have a similar effect. Alternative possibilities for these findings are that Th1 cells also induce LV diastolic dysfunction and chamber dilation but that these only become apparent after durations of pressure overload longer than the time we studied, or that mechanisms other than those mediated by Th1 cells induce diastolic dysfunction and chamber dilation. These possibilities need to be further investigated.

Our studies also demonstrate that transfer of Th1 cells induces a shift in expression of the LV MHC-α isoform, normally expressed in the adult heart, to MHC-β, the fetal isoform only reexpressed in the adult in the setting of pathological cardiac remodeling (Nevers et al., 2015; Salvador et al., 2016). This is also dependent on IFN-γ, as similarly activated IFN-$\gamma^{-/-}$ Th cells did not have that effect. Our data showing that other fetal genes such as Nppa and Nppa, which become reexpressed in pathological hypertrophy, are increased in TCR-$\alpha^{-/-}$ mice AT with Th1 cells or with IFN-$\gamma^{-/-}$ Th cells, but not with naive T cells, support a selective role of IFN-γ on T cell–induced cardiomyocyte MHC isoform switching, not regulating other fetal genes. Although both MHC isoform switch and expression of *Nppa* and *Nppb* serve as markers of pathological remodeling, fetal isoform switch of MHC, but not *Nppa* or *Nppb*, is also known to contribute to systolic and diastolic dysfunction in the cardiomyocyte. Our findings that IFN-$\gamma^{-/-}$ Th cells do not induce MHC isoform switch in TCR-$\alpha^{-/-}$ TAC mice therefore agree with our in vivo findings showing that AT of IFN-$\gamma^{-/-}$ Th cells does not induce the negative functional effects that WT Th1 cells do after AT.

The lack of TAC-induced cardiac hypertrophy in TCR-$\alpha^{-/-}$ mice is striking and also occurs in $CD4^+$-deficient mice (MHC-$II^{-/-}$), whereas it does not occur in WT mice depleted of T cells (Laroumanie et al., 2014; Nevers et al., 2015) or, as we report here, in TCR-$\alpha^{-/-}$ mice reconstituted with naive, Th1, or IFN-$\gamma^{-/-}$ Th cells, suggesting that cardiac hypertrophy is independent of IFN-γ produced by T cells. IFN-γ has been shown to play a role in cardiac hypertrophy in a mouse model of hypertension (Markó et al., 2012), and our data support that such protection may be achieved by IFN-γ from a different cell source other than Th1 cells. Although LV chamber wall thickness only achieved statistical significance in mice receiving Th1 cells, there was a trend toward increased end diastolic diameter in all the AT groups compared with the TCR$^{-/-}$ TAC mice. We interpret these results to support that the hypertrophy observed in TCR-$\alpha^{-/-}$ TAC mice after AT is a function of both concentric and eccentric hypertrophy.

Our data delving into the mechanism of adhesion of Th1 cells to the CFB is of significant interest, as one could speculate that specifically inhibiting such interaction could reduce the profibrotic effects of activated CFB in pathological cardiac remodeling and HF. Our candidate approach focused

mice per group). *, P < 0.05, ANOVA test. (F) Representative immunohistochemistry staining of $CD4^+$ T cells in control (no AT) and TCR-$\alpha^{-/-}$ mice reconstituted with the indicated T cells. Arrows point to positive $CD4^+$ T cells. (G) Quantification of $CD4^+$ cells in the LV of TCR-$\alpha^{-/-}$ control (no AT) or recipients of the indicated T cells. Whole LV sections from n = 6–8 mice per group were analyzed for T cell presence. *, P < 0.05, ANOVA test. (H–J) qRT-PCR of Tbet (H), IL-6 (I), and IL-1β (J) in the LV of TCR-$\alpha^{-/-}$ control (no AT) or recipients of the indicated T cells. n = 6–8 mice per group; *, P < 0.05, ANOVA test. Bars, 50 µm. Error bars represent mean ± SD. *, P < 0.05. ND, not detected; ns, not significant.

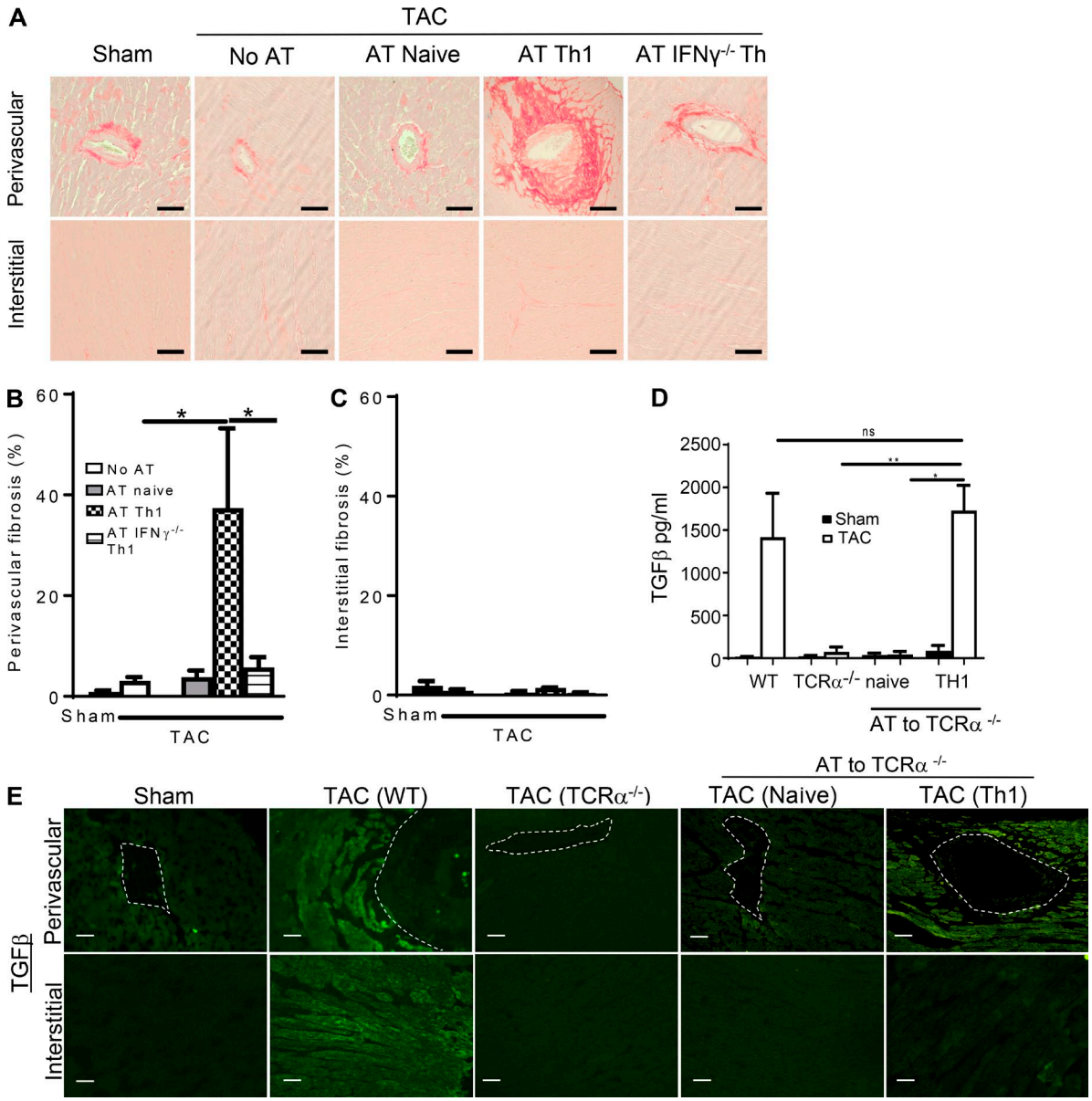

Figure 6. **TCR-$\alpha^{-/-}$ mice have increased perivascular fibrosis after AT of Th1 cells in response to TAC.** (A) Representative picrosirius red staining to identify collagen deposition in the LV after 4 wk of sham or TAC surgery in TCR-$\alpha^{-/-}$ control mice (no AT) or recipients of the indicated T cells. (B) Quantification of perivascular and (C) interstitial fibrosis. Four fields of view for each mouse quantified; n = 6–8 mice per group; *, $P < 0.05$, ANOVA test. (D) Quantification of serum TGF-β by ELISA. n = 6–8 mice per group; *, $P < 0.05$, ANOVA test. (E) Immunofluorescence of TGF-β in the LV of control sham, WT, TCR-$\alpha^{-/-}$ mice or TCR-$\alpha^{-/-}$ mice reconstituted with naive or Th1 cells. Dotted lines surround the vascular lumen in the LV. Representative images of n = 6–8 mice per group are shown. Bars, 50 µm. Error bars represent mean ± SD. Statistical significance is shown as *, $P < 0.05$; **, $P < 0.01$; ns, not significant.

on classic adhesion molecules that are expressed by CFB (Turner et al., 2011), and in their integrin ligands expressed on activated T cells. We interpret our results to identify α4 integrin in Th1 cells as a critical mediator of their adhesion to CFB and, in contrast, to indicate that CFB ICAM-1 is dispensable for Th1 CFB adhesion. This is in line with our previous work indicating a role for ICAM-1 in T cell recruitment to the heart and CF in response to TAC that was independent of ICAM-1 expression on CFB in vitro (Salvador et al., 2016). Small molecule inhibitors for integrins such as αvβ1, expressed on CFB but not implicated in leukocyte adhesion, are promising in treating liver and pulmonary fibrosis (Wipff et al., 2007; Reed et al., 2015). Our data suggest the intriguing possibility of similarly targeting α4 integrins in established HF, once T cells are infiltrated in the heart, to prevent the progression of CF.

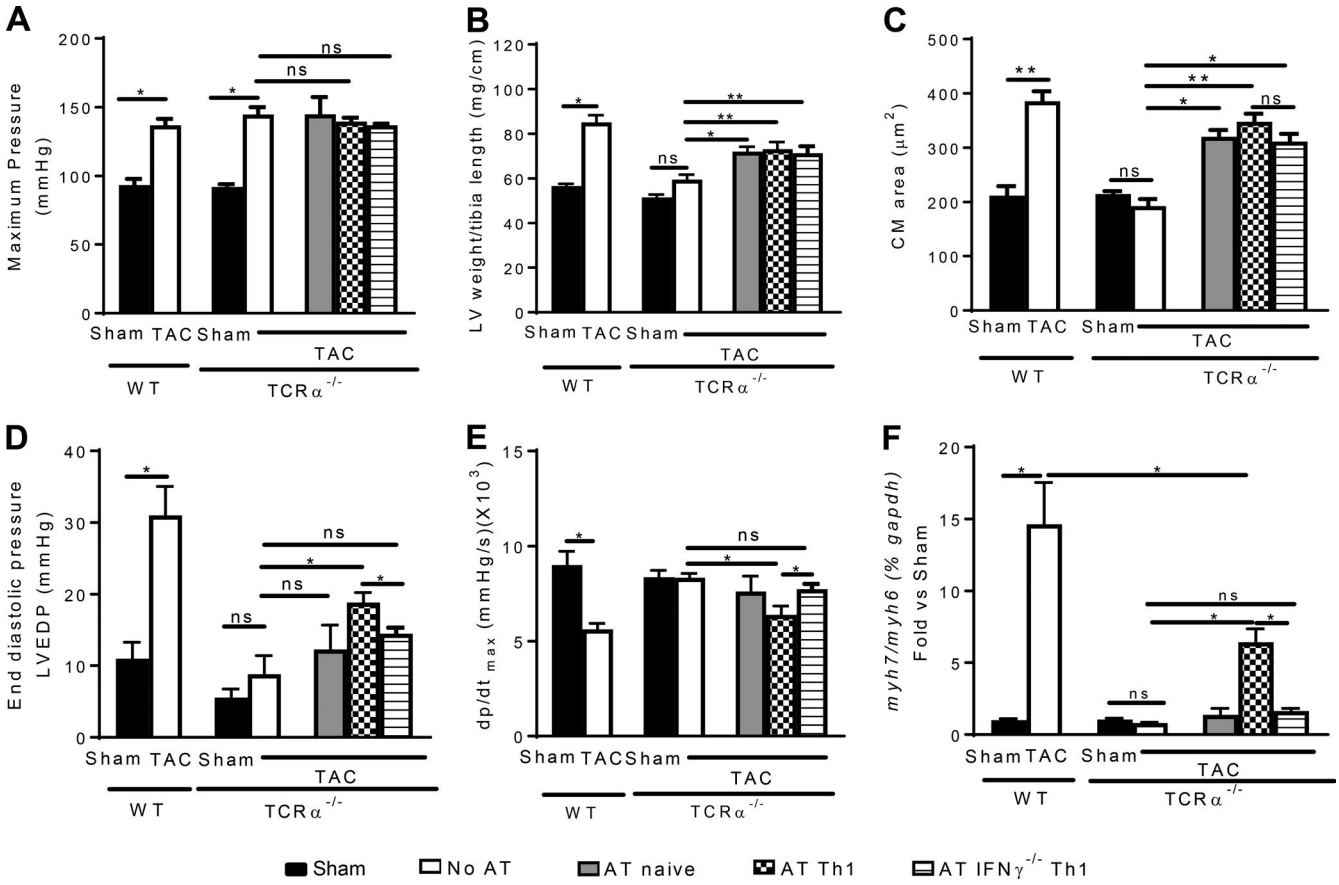

Figure 7. **AT of Th1 cells into TCR-α$^{-/-}$ TAC mice partially induces cardiac dysfunction.** Hemodynamic analysis showing the (A) maximum pressure. (B) LV hypertrophy was analyzed by the LV weight which was normalized to the tibia length. (C) Cardiomyocyte size was determined in LV cross sections. (D and E) Hemodynamic analysis demonstrating the end diastolic pressure (D) and contractile function (E) in WT, TCR-α$^{-/-}$ control mice (no AT) or TCR-α$^{-/-}$ recipients of the indicated T cells, harvested 4 wk after sham or TAC surgery. (F) qRT-PCR of the ratio of MyHCβ/α in the LV in the indicated mice. Error bars represent mean ± SD. Statistical significance is shown as *, P ≤ 0.05; **, P < 0.01; ANOVA test. *n* = 6–8 mice per group. ns, not significant.

Table 1. **Characterization of cardiac function in WT, in TCR-α$^{-/-}$, and in TCR-α$^{-/-}$ mice after AT of naive, Th1, or IFN-γ$^{-/-}$ Th cells 4 wk after sham or TAC**

Parameters	WT sham	WT TAC	TCR-α$^{-/-}$ Sham	TCR-α$^{-/-}$ TAC	TCR-α$^{-/-}$ TAC AT Naive	TCR-α$^{-/-}$ TAC AT Th1	TCR-α$^{-/-}$ TAC AT IFN-γ$^{-/-}$Th
Total mouse weight (g)/tibia length (mm)	1.45 ± 0.02	1.43 ± 0.02	1.45 ± 0.03	1.49 ± 0.04	1.46 ± 0.04	1.51 ± 0.01	1.48 ± 0.03
Lung weight (mg)/tibia length (cm)	91.77 ± 2	123 ± 9[a]	87.33 ± 3	88.11 ± 0	92.39 ± 2	92.32 ± 1	92.41 ± 2
Fractional shortening (%)	39.54 ± 4.036	23.80 ± 2.29[a]	30.92 ± 3.22	38.46 ± 4.10	31.25 ± 3.36	32.24 ± 3.87	30.88 ± 3.90
Anterior wall thickness (mm)	0.87 ± 0.03	1.08 ± 0.08[a]	0.75 ± 0.02	0.87 ± 0.03	0.83 ± 0.14	1.10 ± 0.11[a,b]	0.90 ± 0.10
Posterior wall thickness (mm)	0.94 ± 0.05	1.3 ± 0.07[a]	0.73 ± 0.03	1.01 ± 0.12	0.83 ± 0.14	1.02 ± 0.07[c]	0.87 ± 0.08
End diastolic diameter (mm)	3.49 ± 0.08	3.99 ± 0.15[a]	4.01 ± 0.12	3.9 ± 0.22	4.16 ± 0.16	3.97 ± 0.18	4.08 ± 0.12
End systolic diameter (mm)	2.11 ± 0.16	3.04 ± 0.17[d]	2.77 ± 0.20	2.60 ± 0.28	2.86 ± 0.23	2.69 ± 0.24	2.82 ± 0.17
dp/dt min (mm Hg/s)	−8.28 ± 0.86	−5.61 ± 0.68[a]	−7.89 ± 0.39	−8.00 ± 1.06	−8.76 ± 1.06	−6.67± 0.70	−7.61 ± 1.12

Values are means ± SEM.
[a]P < 0.05, 4 wk of TAC versus sham.
[b]P < 0.05, 4 wk TAC AT TCR-α$^{-/-}$ versus TAC TCR-α$^{-/-}$.
[c]P < 0.01, 4 wk TAC AT TCR-α$^{-/-}$ versus TAC TCR-α$^{-/-}$.
[d]P < 0.01, 4 wk of TAC versus sham.

From the immunological perspective, the prevailing paradigm holds that T cells become activated in response to antigen followed by a secondary costimulatory signal (Harding et al., 1992), but recent emerging evidence suggests that T cells can also be activated through nonclassic antigen-mediated pathways (Rahman et al., 2009). Oxidized antigens have been recently described to induce T cell activation in a model of angiotensin II–induced hypertension (Kirabo et al., 2014; Wu et al., 2016), but, as it occurs in TAC-induced HF, the specific nature of the antigen or antigens remains elusive. Indirect evidence points toward cardiac Ag-specific T cell activation as OT-II mice, exclusively responding to OVA, and CD28/B7$^{-/-}$ mice lacking costimulatory signals, do not develop HF or CF in response to TAC (Laroumanie et al., 2014; Wang et al., 2016), and this possibility has also been suggested in later stages of TAC-induced HF (Wang et al., 2016). Our data demonstrating that nonantigen-specific Th1 cells partially mediate cardiac dysfunction is in support of this latter mechanism. Additional supporting evidence comes from the fact that naive T cells do not become activated or infiltrate the LV in recipient TCR-α$^{-/-}$ mice in response to TAC, suggesting naive T cells do not sufficiently respond to antigen in the host in response to TAC. Our results document the biological importance of Th1 cells generated in a nonantigen-specific way, which are sufficient to traffic to the heart and modulate LV inflammation, perivascular fibrosis and some aspects of cardiac dysfunction. We can speculate that cardiac antigens are needed to sustain T cell activation in the heart, interstitial fibrosis, and the progression of cardiac pathology and HF. This remains an area of current and future investigation.

In summary, our data demonstrate a role for IFN-γ–producing Th1 cells in orchestrating CF through mechanisms that involve T cell integrin-mediated adhesion with CFB and subsequent TGF-β release. Our results, together with the growing body of literature evaluating the adaptive immune response in heart failure, enhance our global understanding of effector T cell–mediated pathological remodeling and HF and help resolve a paradox in the field for a role of IFN-γ in heart failure, while opening a possibility of interfering with a T cell–specific subset and integrin-mediated adhesion toward a less proinflammatory and more antifibrotic phenotype.

MATERIALS AND METHODS

Mice

WT (C57BL/6) and TCR-α$^{-/-}$ mice were bred and maintained under pathogen-free conditions. IFN-γ$^{-/-}$ mice were purchased from the Jackson Laboratory. All procedures conformed to the animal welfare regulations of Tufts University and were approved by the Tufts University Institutional Animal Care and Use Committee. All mice used for experiments were 8–14 wk old.

Animal model

The mouse model of TAC was used to induce pressure overload in the LV as previously described (Rockman et al., 1991; Patten et al., 2008; Blanton et al., 2012; Salvador et al., 2016). Sham mice were used as control in all studies and were operated as TAC mice except for the suture tied around the needle to constrict the aorta.

Preparation of adult CFBs

Adult WT mice (6–8 wk old) were anesthetized. Hearts were excised, minced, washed and then subjected to digestion at 37°C for 30 min with agitation in a mixture of 0.25% trypsin and 5 mg/ml liberase TL (Roche). Digested tissue was then centrifuged at 1500 rpm for 5 min and the pellet resuspended into fibroblasts culture media ([FBM] 10% normal bovine serum and 100 U/ml penicillin/streptomycin) and plated on 1% gelatin coated plates for 2 h at 37°C with 5% CO_2. At the end of this period, the unattached cells were discarded, and attached cells were grown in fibroblast culture medium. Once confluent, CFBs were trypsinized but not scrapped, and thus negatively selecting for potential contaminating macrophages adhered to the plate, and trypsin detached cells passaged to use in co-culture experiments. CFB were used between passages 1–2. FACS staining with CD45, CD11b, CD64 was performed before and after plating to determine the CFB purity (only 0.36% of CD45$^+$ T cells in cultured CFB (8 d) compared with a mean of 36% of CD45$^+$ at the day 0 of the culture). F4/80 antibody further determined the lack of contamination by macrophages in each CFB culture. Bone marrow macrophages were isolated from mice tibias and femurs, stimulated with LPS (5 μg/ml) as described (Salvador et al., 2016), and used as a positive control for F4/80 staining. Where indicated, CFBs were incubated with clodronate liposomes (50 μl/ml) for 48 h before the T cell–CFB co-culture was established, using the macrophage depletion kit (Encapsula NanoSciences) using splenocytes as a positive control for macrophage deletion (Fig. S3).

Preparation of T cell subsets for in vitro co-cultures and for in vivo AT

Where indicated, CD4$^+$ T cells were isolated from the mLNs of WT mice 4 wk after sham or TAC surgery by positive selection with magnetic beads (Milteny) and used in in vitro co-cultures right after isolation. Naive CD4$^+$ T cells were isolated from the spleen and LNs of 8–12 wk WT mice and used directly in co-cultures or adoptively transferred into TCR-α$^{-/-}$ recipient mice. Th1 cells were differentiated from the WT naive T cells by anti-CD3 and anti-CD28 stimulation in the presence of IL-12, IL-2, and anti–IL-4, and expanded with IL-2 at day 3 for two additional days, as previously described (Alcaide et al., 2012; Velázquez et al., 2016). IFN-γ$^{-/-}$ Th cells were generated from IFN-γ$^{-/-}$ naive T cells under the same conditions as WT Th1 cells. Th1 and IFN-γ$^{-/-}$ Th were harvested on day 5 after CD4$^+$ T cell isolation and used in co-culture experiments or adoptively transferred intraperitoneally at a concentration of 10^7 cells/500 μl PBS into TCR-α$^{-/-}$ recipient mice. In the AT experiments, comparisons were established between TCR-α$^{-/-}$ TAC mice that did not receive any T

cells (no AT) and TCR-$\alpha^{-/-}$ TAC mice receiving the different T cell types, unless otherwise indicated.

In vitro co-culture of fibroblasts and CD4 T cells

Fibroblasts were distributed in 6-well plates, glass coverslips, or in 0.4-µm pore diameter 12-well Transwell plates coated with 1% gelatin and cultured overnight in FBM supplemented with 10% (vol/vol) FCS (500,000 cells in 1 ml of medium/well). Half the medium was then removed and the CD4 T cell suspension generated as indicated in the section above (100,000 cells in 0.5 ml FBM) was added to each well or to the upper well of the Transwell, where indicated. T cells and CFB were co-cultured overnight at 37°C with 5% CO_2. Where indicated, T cells were labeled with anti-CD4–Alexa Fluor 488 Ab, 30 min at room temperature, before being added to the CFB plates or Transwells. In some experiments, adherent Th1 cells to the CFB were detached using gentle EDTA (5 mM) washes. Detached Th1 cells and CFBs detached of T cells were collected and stained with anti–TGF-β for FACS analysis. Where indicated, CFBs detached of T cells were stained with anti–TGF-β by immunofluorescence. Photomicrographs were taken before and after washing cells. Cells were fixed for immunofluorescence staining after washing.

Neutralization of TGF-β and α4 integrin

5 µg/ml anti–TGF-β (clone1D11, R&D) was added to adult CFB cells 1 h before adding Th1 cells at a 5:1 (CFB/T cell) ratio. CFB/T cell co-culture with or without anti–TGF-β was incubated overnight. 1D11 is a mouse mAb that specifically neutralizes the biological activity of TGF-β1, TGF-β2, and TGF-β3 both in vitro and in vivo (Dasch et al., 1989). A total of 20 µg/ml α4 integrin (CD49d; clone 9C10, BioLegend) was added to Th1 cells for 30 min before overnight co-culture with CFB. Isotype rat IgG2a was used as control.

Immunofluorescence

CFBs were cultured in FGM_2 on 1% gelatin-coated glass coverslips within a 6-well plate until confluent. They were then deprived of serum for 24 h. T cell subsets were labeled with $CD4^+$–Alexa Fluor 488 or remained unlabeled and added to the culture medium in concentrations as indicated overnight. At the end of each treatment, cell layers were washed twice with PBS and permeabilized in ice-cold acetone for 10 min. Nonspecific binding was prevented by incubation with DPBS + 0.1 mg/ml salmon DNA, 1% goat serum, and 1% horse serum for 1 h. Cells were incubated with specific antibodies at 1:250 dilution. The cells were then incubated at 4°C overnight and washed three times with PBS. As negative controls, parallel slides were incubated with no primary antibody. Alexa Fluor 568–conjugated goat anti–mouse or goat pAB to α chicken IgY Alexa Fluor 488 was used as a secondary antibody. Visualization was performed with a Nikon Ti inverted fluorescent microscope. Quantification of α-SMA fluorescence intensity was performed using National Institutes of Health ImageJ software.

RNA extraction and real-time quantitative PCR

Total RNAs were Trizol-extracted from mouse heart LV tissues or CFB. RNA was reverse-transcribed using the ThermoScript RT-PCR system according to the manufacturer's instructions (Invitrogen). Real-time quantitative PCR reactions involved use of SYBR Green PCR mix (Applied Biosystems). Samples were quantified in triplicate using 40 cycles performed at 94°C for 30 s, 60°C for 45 s, and 72°C for 45 s using the ABI Prism 7900 Sequence Detection System. The housekeeping gene GAPDH was used as control. The sequences of the primers used were as follows: *myh6*: forward 5′-TGAGCCTTGGATTCTCAAACGT-3′, reverse 5′-AGGTGGCTCCGAGAAAGGAA-3′; *myh7*: forward 5′-GCTGTGCTTTGAGAACTGTG-3′, reverse 5′-GTGAGG TCCTTGCCTACTTG-3′; *il1b*: forward 5′-TGATGGATG CTACCAAACTGG-3′, reverse 5′-TTCATGTACTCC AGGTAGCTATGG-3′; *il6*: forward 5′-GCACAGAAAGCA TGACCCG-3′, reverse 5′-GCCCCCCATCTTTTGGG-3′; *Tbx21*: forward 5′-CAACAACCCCTTTGCCAAAG-3′, reverse 5′-TCCCCCAAGCAGTTGACAGT-3′; *Ifng*: forward 5′-AACGCTACACACTGCATCTTGG-3′, reverse 5′-GCCGTGGCAGTAACAGCC-3′; *Il4*: forward 5′-TCG GCATTTTGAACGAGGTC-3′, reverse 5′-GAAAAGCCC GAAAGAGTCTC-3′; *Il5*: forward 5′-TCACCGAGCTCT GTTGACAA-3′, reverse 5′-CCACACTTCTCTTTTTGG CG-3′; *nppb*: forward 5′-GAGAGACGGCAGTGCTTC TAGGC-3′, reverse 5′-CGTGACACACCACAAGGGCTT AGG -3′; *nppa*: forward 5′-AAGGGTCCCTCTGGAGAA CC-3′, reverse 5′-TCTAGAGCCAGGGAGACCCA-3′.

Histology

The ventricles were fixed in 10% formalin, embedded in paraffin, and cut into 5-µm sections. Hematoxylin and eosin or picrosirius red staining was performed as described (Nevers et al., 2015). Immunohistochemistry was performed in LV frozen sections that were incubated with primary antibody against CD4 (1:500 dilution) for 2 h followed with incubation of secondary antibody goat antirat biotinylated as described (Nevers et al., 2015; Salvador et al., 2016). In some cases, LV frozen sections were stained for immunofluorescence using anti–TGF-β (chicken polyclonal, Abcam). Cardiomyocyte cross-sectional area was quantified by tracing the outline of 10–15 myocytes in each section (Nevers et al., 2015).

Flow cytometry

Flow cytometry was used to analyze the immune cellular profile present in lymphoid tissues, to evaluate the presence of $F4/80^+$ macrophages in CFB preparations, to evaluate the expression of IFN-γ by Th cells, and to determine the source of TGF-β in vitro. The data were acquired on an LSRII (Becton Dickinson) and analyzed using FlowJo software. All antibodies were from Biolegend: anti-CD4-FITC (clone GK1.5), anti-IL-17A-APC (clone TC11-18H 10.1), anti-IFN-γ-PE (XMG 1.2), anti-Foxp3-PE (MF14), anti-F4/80-APC (BM8), anti-TGF-β1 (clone TN7-1B4), anti-CD45.2-brilliant violet

711 (clone 104), anti-CD64-PE (clone X54-5/7.1) and anti-CD11b-APC (clone M1/70).

TGF-β ELISA

TGF-β1 protein was quantitated by ELISA according to the manufacturer's instructions (R&D Systems), on supernatants of co-culture of CFB with naive or Th1 cells, with or without TGF-β blocking antibody. Circulating TGF-β was also measured from sham and TAC C57/BL6 mice, TCR-$\alpha^{-/-}$ mice, or TCR-$\alpha^{-/-}$ mice adoptively transferred with naive or Th1 cells.

In vivo echocardiography

In vivo transthoracic echocardiography was assessed in slightly sedated mice as described (Blanton et al., 2012). M-mode and two-dimensional images were obtained from the short-axis view (Patten et al., 2008). All analyses were performed blindly.

Hemodynamics

A pressure volume transducer catheter was introduced into the LV through the carotid artery of anesthetized mice and used to assess LV function as previously described (Blanton et al., 2012). Absolute volume was calibrated by saline injection parallel conductance method and data evaluated at steady state (Blanton et al., 2012). Data were digitized and analyzed using custom software (EMKA version 2.1.10).

Statistics

All results are presented as mean ± SD unless otherwise indicated. Two group comparisons were analyzed by Student *t*-test and Mann-Whitney nonparametric test to adjust for nonequal Gaussian distribution among groups. Multiple group comparisons were performed by one- or two-way ANOVA and Bonferroni posttest where indicated. The difference was considered statistically significant at *, $P \leq 0.05$; **, $P \leq 0.01$; and ***, $P \leq 0.005$. All statistical analyses were performed using GraphPad Prism.

Online supplemental information.

Fig. S1 shows FACS staining of IL-17A and Foxp3 in the mLNs of sham and TAC WT mice. Fig. S2 shows FACS staining of IFN-γ in T cells used in co-cultures and AT. Fig. S3 shows α-SMA immunofluorescence staining in clodronate-treated CFB co-cultured with Th1 cells. Fig. S4 shows gene expression of cardiac hypertrophy genes.

ACKNOWLEDGMENTS

These studies were supported by National Institutes of Health grants NIH RO1 HL123658 (to P. Alcaide), NIH 1KL2TR001063-01 (to R.M. Blanton), NIH R01HL131831 (to R.M. Blanton), NIH T32 HL 69770 (to T. Nevers), and NIH T32AI007077-34 (to N. Ngwenyama) and by American Heart Association Grant in Aid AHA GIA 13GRNT 14560068 (P. Alcaide).

The authors declare no competing financial interests.

Author contributions: T. Nevers designed and performed all the experiments and wrote the manuscript. A.M. Salvator performed the quantitative PCR studies, generated WT and IFN-$\gamma^{-/-}$ Th cells, and performed AT studies with such cells. F. Velazquez performed T cell isolation in some of the in vivo studies and Transwell assays. M. Aronovitz performed the TAC surgery and catheterization for the hemodynamic studies. N. Ngwenyama performed Transwell and co-culture studies with WT and IFN-$\gamma^{-/-}$ Th cells as well as the EDTA detachment and clodronate liposome experiments with the corresponding FACS and immunofluorescence. F.J. Carrillo-Salinas performed quantitative PCR studies and histology in tissues from mice receiving IFN-$\gamma^{-/-}$ Th cells. R.M. Blanton did the echocardiography measurements and hemodynamic analysis. P. Alcaide overviewed the design and interpretation of all studies and wrote the manuscript.

Submitted: 24 October 2016
Revised: 13 June 2017
Accepted: 21 August 2017

REFERENCES

Afanasyeva, M., D. Georgakopoulos, D. Fairweather, P. Caturegli, D.A. Kass, and N.R. Rose. 2004. Novel model of constrictive pericarditis associated with autoimmune heart disease in interferon-gamma-knockout mice. *Circulation*. 110:2910–2917. https://doi.org/10.1161/01.CIR.0000147538.92263.3A

Alcaide, P., E. Maganto-Garcia, G. Newton, R. Travers, K.J. Croce, D.X. Bu, F.W. Luscinskas, and A.H. Lichtman. 2012. Difference in Th1 and Th17 lymphocyte adhesion to endothelium. *J. Immunol.* 188:1421–1430. https://doi.org/10.4049/jimmunol.1101647

Anderson, K.R., M.G. Sutton, and J.T. Lie. 1979. Histopathological types of cardiac fibrosis in myocardial disease. *J. Pathol.* 128:79–85. https://doi.org/10.1002/path.1711280205

Bansal, S.S., M.A. Ismahil, M. Goel, B. Patel, T. Hamid, G. Rokosh, and S.D. Prabhu. 2017. Activated T Lymphocytes are Essential Drivers of Pathological Remodeling in Ischemic Heart Failure. *Circ Heart Fail.* 10:e003688. https://doi.org/10.1161/CIRCHEARTFAILURE.116.003688

Blanton, R.M., E. Takimoto, A.M. Lane, M. Aronovitz, R. Piotrowski, R.H. Karas, D.A. Kass, and M.E. Mendelsohn. 2012. Protein kinase g iα inhibits pressure overload-induced cardiac remodeling and is required for the cardioprotective effect of sildenafil in vivo. *J. Am. Heart Assoc.* 1:e003731. https://doi.org/10.1161/JAHA.112.003731

Border, W.A., and N.A. Noble. 1994. Transforming growth factor beta in tissue fibrosis. *N. Engl. J. Med.* 331:1286–1292. https://doi.org/10.1056/NEJM199411103311907

Borthwick, L.A., T.A. Wynn, and A.J. Fisher. 2013. Cytokine mediated tissue fibrosis. *Biochim. Biophys. Acta.* 1832:1049–1060. https://doi.org/10.1016/j.bbadis.2012.09.014

Braunwald, E. 2013. Heart failure. *JACC Heart Fail.* 1:1–20. https://doi.org/10.1016/j.jchf.2012.10.002

Bujak, M., and N.G. Frangogiannis. 2007. The role of TGF-beta signaling in myocardial infarction and cardiac remodeling. *Cardiovasc. Res.* 74:184–195. https://doi.org/10.1016/j.cardiores.2006.10.002

Bujak, M., M. Dobaczewski, C. Gonzalez-Quesada, Y. Xia, T. Leucker, P. Zymek, V. Veeranna, A.M. Tager, A.D. Luster, and N.G. Frangogiannis. 2009. Induction of the CXC chemokine interferon-gamma-inducible protein 10 regulates the reparative response following myocardial infarction. *Circ. Res.* 105:973–983. https://doi.org/10.1161/CIRCRESAHA.109.199471

Burzyn, D., W. Kuswanto, D. Kolodin, J.L. Shadrach, M. Cerletti, Y. Jang, E. Sefik, T.G. Tan, A.J. Wagers, C. Benoist, and D. Mathis. 2013. A special population of regulatory T cells potentiates muscle repair. *Cell.* 155:1282–1295. https://doi.org/10.1016/j.cell.2013.10.054

Chaturvedi, R.R., T. Herron, R. Simmons, D. Shore, P. Kumar, B. Sethia, F. Chua, E. Vassiliadis, and J.C. Kentish. 2010. Passive stiffness of myocardium from congenital heart disease and implications for diastole.

Circulation. 121:979–988. https://doi.org/10.1161/CIRCULATIONAHA.109.850677

Chen, B., and N.G. Frangogiannis. 2016. Macrophages in the Remodeling Failing Heart. *Circ. Res.* 119:776–778. https://doi.org/10.1161/CIRCRESAHA.116.309624

Costa, R.A., V. Ruiz-de-Souza, G.M. Azevedo Jr., E. Gava, G.T. Kitten, N.M. Vaz, and C.R. Carvalho. 2011. Indirect effects of oral tolerance improve wound healing in skin. *Wound Repair Regen*. 19:487–497. https://doi.org/10.1111/j.1524-475X.2011.00700.x

Dasch, J.R., D.R. Pace, W. Waegell, D. Inenaga, and L. Ellingsworth. 1989. Monoclonal antibodies recognizing transforming growth factor-beta. Bioactivity neutralization and transforming growth factor beta 2 affinity purification. *J. Immunol*. 142:1536–1541.

Fairweather, D., S. Frisancho-Kiss, S.A. Yusung, M.A. Barrett, S.E. Davis, S.J. Gatewood, D.B. Njoku, and N.R. Rose. 2004. Interferon-gamma protects against chronic viral myocarditis by reducing mast cell degranulation, fibrosis, and the profibrotic cytokines transforming growth factor-beta 1, interleukin-1 beta, and interleukin-4 in the heart. *Am. J. Pathol*. 165:1883–1894. https://doi.org/10.1016/S0002-9440(10)63241-5

Fan, D., A. Takawale, J. Lee, and Z. Kassiri. 2012. Cardiac fibroblasts, fibrosis and extracellular matrix remodeling in heart disease. *Fibrogenesis Tissue Repair.* 5:15. https://doi.org/10.1186/1755-1536-5-15

Frangogiannis, N.G. 2004. Chemokines in the ischemic myocardium: from inflammation to fibrosis. *Inflamm. Res.* 53:585–595. https://doi.org/10.1007/s00011-004-1298-5

Frangogiannis, N.G., C.W. Smith, and M.L. Entman. 2002. The inflammatory response in myocardial infarction. *Cardiovasc. Res.* 53:31–47. https://doi.org/10.1016/S0008-6363(01)00434-5

Fukasawa, H., T. Yamamoto, H. Suzuki, A. Togawa, N. Ohashi, Y. Fujigaki, C. Uchida, M. Aoki, M. Hosono, M. Kitagawa, and A. Hishida. 2004. Treatment with anti-TGF-beta antibody ameliorates chronic progressive nephritis by inhibiting Smad/TGF-beta signaling. *Kidney Int*. 65:63–74. https://doi.org/10.1111/j.1523-1755.2004.00393.x

Germain, R.N. 1994. MHC-dependent antigen processing and peptide presentation: providing ligands for T lymphocyte activation. *Cell*. 76:287–299. https://doi.org/10.1016/0092-8674(94)90336-0

Gurujeyalakshmi, G., and S.N. Giri. 1995. Molecular mechanisms of antifibrotic effect of interferon gamma in bleomycin-mouse model of lung fibrosis: downregulation of TGF-beta and procollagen I and III gene expression. *Exp. Lung Res.* 21:791–808. https://doi.org/10.3109/01902149509050842

Han, Y.L., Y.L. Li, L.X. Jia, J.Z. Cheng, Y.F. Qi, H.J. Zhang, and J. Du. 2012. Reciprocal interaction between macrophages and T cells stimulates IFN-γ and MCP-1 production in Ang II-induced cardiac inflammation and fibrosis. *PLoS One.* 7:e35506. https://doi.org/10.1371/journal.pone.0035506

Harding, F.A., J.G. McArthur, J.A. Gross, D.H. Raulet, and J.P. Allison. 1992. CD28-mediated signalling co-stimulates murine T cells and prevents induction of anergy in T-cell clones. *Nature.* 356:607–609. https://doi.org/10.1038/356607a0

Hirahara, K., and T. Nakayama. 2016. CD4+ T-cell subsets in inflammatory diseases: beyond the Th1/Th2 paradigm. *Int. Immunol*. 28:163–171. https://doi.org/10.1093/intimm/dxw006

Hofmann, U., N. Beyersdorf, J. Weirather, A. Podolskaya, J. Bauersachs, G. Ertl, T. Kerkau, and S. Frantz. 2012. Activation of CD4+ T lymphocytes improves wound healing and survival after experimental myocardial infarction in mice. *Circulation*. 125:1652–1663. https://doi.org/10.1161/CIRCULATIONAHA.111.044164

Kai, H., T. Mori, K. Tokuda, N. Takayama, N. Tahara, K. Takemiya, H. Kudo, Y. Sugi, D. Fukui, H. Yasukawa, et al. 2006. Pressure overload-induced transient oxidative stress mediates perivascular inflammation and cardiac fibrosis through angiotensin II. *Hypertens. Res.* 29:711–718. https://doi.org/10.1291/hypres.29.711

Kanellakis, P., T.N. Dinh, A. Agrotis, and A. Bobik. 2011. $CD4^+CD25^+Foxp3^+$ regulatory T cells suppress cardiac fibrosis in the hypertensive heart. *J. Hypertens.* 29:1820–1828. https://doi.org/10.1097/HJH.0b013e328349c62d

Kirabo, A., V. Fontana, A.P. de Faria, R. Loperena, C.L. Galindo, J. Wu, A.T. Bikineyeva, S. Dikalov, L. Xiao, W. Chen, et al. 2014. DC isoketal-modified proteins activate T cells and promote hypertension. *J. Clin. Invest*. 124:4642–4656. https://doi.org/10.1172/JCI74084

Laroumanie, F., V. Douin-Echinard, J. Pozzo, O. Lairez, F. Tortosa, C. Vinel, C. Delage, D. Calise, M. Dutaur, A. Parini, and N. Pizzinat. 2014. CD4+ T cells promote the transition from hypertrophy to heart failure during chronic pressure overload. *Circulation*. 129:2111–2124. https://doi.org/10.1161/CIRCULATIONAHA.113.007101

Markó, L., H. Kvakan, J.K. Park, F. Qadri, B. Spallek, K.J. Binger, E.P. Bowman, M. Kleinewietfeld, V. Fokuhl, R. Dechend, and D.N. Müller. 2012. Interferon-γ signaling inhibition ameliorates angiotensin II-induced cardiac damage. *Hypertension*. 60:1430–1436. https://doi.org/10.1161/HYPERTENSIONAHA.112.199265

Mombaerts, P., A.R. Clarke, M.A. Rudnicki, J. Iacomini, S. Itohara, J.J. Lafaille, L. Wang, Y. Ichikawa, R. Jaenisch, M.L. Hooper, et al. 1992. Mutations in T-cell antigen receptor genes alpha and beta block thymocyte development at different stages. *Nature.* 360:225–231. https://doi.org/10.1038/360225a0

Mozaffarian, D., E.J. Benjamin, A.S. Go, D.K. Arnett, M.J. Blaha, M. Cushman, S.R. Das, S. de Ferranti, J.P. Després, H.J. Fullerton, et al. Stroke Statistics Subcommittee. 2016. Executive Summary: Heart Disease and Stroke Statistics—2016 Update: A Report From the American Heart Association. *Circulation*. 133:447–454. https://doi.org/10.1161/CIR.0000000000000366

Murray, L.A., Q. Chen, M.S. Kramer, D.P. Hesson, R.L. Argentieri, X. Peng, M. Gulati, R.J. Homer, T. Russell, N. van Rooijen, et al. 2011. TGF-beta driven lung fibrosis is macrophage dependent and blocked by Serum amyloid P. *Int. J. Biochem. Cell Biol.* 43:154–162. https://doi.org/10.1016/j.biocel.2010.10.013

Nakamura, T., R. Sakata, T. Ueno, M. Sata, and H. Ueno. 2000. Inhibition of transforming growth factor beta prevents progression of liver fibrosis and enhances hepatocyte regeneration in dimethylnitrosamine-treated rats. *Hepatology.* 32:247–255. https://doi.org/10.1053/jhep.2000.9109

Nevers, T., A.M. Salvador, A. Grodecki-Pena, A. Knapp, F. Velázquez, M. Aronovitz, N.K. Kapur, R.H. Karas, R.M. Blanton, and P. Alcaide. 2015. Left Ventricular T-Cell Recruitment Contributes to the Pathogenesis of Heart Failure. *Circ Heart Fail.* 8:776–787. https://doi.org/10.1161/CIRCHEARTFAILURE.115.002225

Nguyen, H., V.L. Chiasson, P. Chatterjee, S.E. Kopriva, K.J. Young, and B.M. Mitchell. 2013. Interleukin-17 causes Rho-kinase-mediated endothelial dysfunction and hypertension. *Cardiovasc. Res.* 97:696–704. https://doi.org/10.1093/cvr/cvs422

Oldroyd, S.D., G.L. Thomas, G. Gabbiani, and A.M. El Nahas. 1999. Interferon-gamma inhibits experimental renal fibrosis. *Kidney Int*. 56:2116–2127. https://doi.org/10.1046/j.1523-1755.1999.00775.x

Patten, R.D., I. Pourati, M.J. Aronovitz, A. Alsheikh-Ali, S. Eder, T. Force, M.E. Mendelsohn, and R.H. Karas. 2008. 17 Beta-estradiol differentially affects left ventricular and cardiomyocyte hypertrophy following myocardial infarction and pressure overload. *J. Card. Fail.* 14:245–253. https://doi.org/10.1016/j.cardfail.2007.10.024

Rahman, A.H., D.K. Taylor, and L.A. Turka. 2009. The contribution of direct TLR signaling to T cell responses. *Immunol. Res.* 45:25–36. https://doi.org/10.1007/s12026-009-8113-x

Reed, N.I., H. Jo, C. Chen, K. Tsujino, T.D. Arnold, W.F. DeGrado, and D. Sheppard. 2015. The αvβ1 integrin plays a critical in vivo role in tissue fibrosis. *Sci. Transl. Med*. 7:288ra79. https://doi.org/10.1126/scitranslmed.aaa5094

Rockman, H.A., R.S. Ross, A.N. Harris, K.U. Knowlton, M.E. Steinhelper, L.J. Field, J. Ross Jr., and K.R. Chien. 1991. Segregation of atrial-specific and inducible expression of an atrial natriuretic factor transgene in an in vivo murine model of cardiac hypertrophy. *Proc. Natl. Acad. Sci. USA.* 88:8277–8281. https://doi.org/10.1073/pnas.88.18.8277

Salvador, A.M., T. Nevers, F. Velázquez, M. Aronovitz, B. Wang, A. Abadía Molina, I.Z. Jaffe, R.H. Karas, R.M. Blanton, and P. Alcaide. 2016. Intercellular Adhesion Molecule 1 Regulates Left Ventricular Leukocyte Infiltration, Cardiac Remodeling, and Function in Pressure Overload-Induced Heart Failure. *J. Am. Heart Assoc.* 5:e003126. https://doi.org/10.1161/JAHA.115.003126

Sandler, N.G., M.M. Mentink-Kane, A.W. Cheever, and T.A. Wynn. 2003. Global gene expression profiles during acute pathogen-induced pulmonary inflammation reveal divergent roles for Th1 and Th2 responses in tissue repair. *J. Immunol.* 171:3655–3667. https://doi.org/10.4049/jimmunol.171.7.3655

Saxena, A., M. Dobaczewski, V. Rai, Z. Haque, W. Chen, N. Li, and N.G. Frangogiannis. 2014. Regulatory T cells are recruited in the infarcted mouse myocardium and may modulate fibroblast phenotype and function. *Am. J. Physiol. Heart Circ. Physiol.* 307:H1233–H1242. https://doi.org/10.1152/ajpheart.00328.2014

Takemasa, A., Y. Ishii, and T. Fukuda. 2012. A neutrophil elastase inhibitor prevents bleomycin-induced pulmonary fibrosis in mice. *Eur. Respir. J.* 40:1475–1482. https://doi.org/10.1183/09031936.00127011

Teekakirikul, P., S. Eminaga, O. Toka, R. Alcalai, L. Wang, H. Wakimoto, M. Nayor, T. Konno, J.M. Gorham, C.M. Wolf, et al. 2010. Cardiac fibrosis in mice with hypertrophic cardiomyopathy is mediated by non-myocyte proliferation and requires Tgf-β. *J. Clin. Invest.* 120:3520–3529. https://doi.org/10.1172/JCI42028

Travers, J.G., F.A. Kamal, J. Robbins, K.E. Yutzey, and B.C. Blaxall. 2016. Cardiac Fibrosis: The Fibroblast Awakens. *Circ. Res.* 118:1021–1040. https://doi.org/10.1161/CIRCRESAHA.115.306565

Turner, N.A., A. Das, D.J. O'Regan, S.G. Ball, and K.E. Porter. 2011. Human cardiac fibroblasts express ICAM-1, E-selectin and CXC chemokines in response to proinflammatory cytokine stimulation. *Int. J. Biochem. Cell Biol.* 43:1450–1458. https://doi.org/10.1016/j.biocel.2011.06.008

Velázquez, F., A. Grodecki-Pena, A. Knapp, A.M. Salvador, T. Nevers, K. Croce, and P. Alcaide. 2016. CD43 Functions as an E-Selectin Ligand for Th17 Cells In Vitro and Is Required for Rolling on the Vascular Endothelium and Th17 Cell Recruitment during Inflammation In Vivo. *J. Immunol.* 196:1305–1316. https://doi.org/10.4049/jimmunol.1501171

Walsh, J.T., S. Hendrix, F. Boato, I. Smirnov, J. Zheng, J.R. Lukens, S. Gadani, D. Hechler, G. Gölz, K. Rosenberger, et al. 2015. MHCII-independent CD4+ T cells protect injured CNS neurons via IL-4. *J. Clin. Invest.* 125:699–714. https://doi.org/10.1172/JCI76210

Wang, H., D. Kwak, J. Fassett, L. Hou, X. Xu, B.J. Burbach, T. Thenappan, Y. Xu, J.B. Ge, Y. Shimizu, et al. 2016. CD28/B7 Deficiency Attenuates Systolic Overload-Induced Congestive Heart Failure, Myocardial and Pulmonary Inflammation, and Activated T Cell Accumulation in the Heart and Lungs. *Hypertension.* 68:688–696. https://doi.org/10.1161/HYPERTENSIONAHA.116.07579

Weber, K.T. 1989. Cardiac interstitium in health and disease: the fibrillar collagen network. *J. Am. Coll. Cardiol.* 13:1637–1652. https://doi.org/10.1016/0735-1097(89)90360-4

Wei, L. 2011. Immunological aspect of cardiac remodeling: T lymphocyte subsets in inflammation-mediated cardiac fibrosis. *Exp. Mol. Pathol.* 90:74–78. https://doi.org/10.1016/j.yexmp.2010.10.004

Wilson, M.S., and T.A. Wynn. 2009. Pulmonary fibrosis: pathogenesis, etiology and regulation. *Mucosal Immunol.* 2:103–121. https://doi.org/10.1038/mi.2008.85

Wipff, P.J., D.B. Rifkin, J.J. Meister, and B. Hinz. 2007. Myofibroblast contraction activates latent TGF-β1 from the extracellular matrix. *J. Cell Biol.* 179:1311–1323. https://doi.org/10.1083/jcb.200704042

Wu, J., M.A. Saleh, A. Kirabo, H.A. Itani, K.R. Montaniel, L. Xiao, W. Chen, R.L. Mernaugh, H. Cai, K.E. Bernstein, et al. 2016. Immune activation caused by vascular oxidation promotes fibrosis and hypertension. *J. Clin. Invest.* 126:1607. https://doi.org/10.1172/JCI87425

Wu, L., S. Ong, M.V. Talor, J.G. Barin, G.C. Baldeviano, D.A. Kass, D. Bedja, H. Zhang, A. Sheikh, J.B. Margolick, et al. 2014. Cardiac fibroblasts mediate IL-17A-driven inflammatory dilated cardiomyopathy. *J. Exp. Med.* 211:1449–1464. https://doi.org/10.1084/jem.20132126

Xia, Y., K. Lee, N. Li, D. Corbett, L. Mendoza, and N.G. Frangogiannis. 2009. Characterization of the inflammatory and fibrotic response in a mouse model of cardiac pressure overload. *Histochem. Cell Biol.* 131:471–481. https://doi.org/10.1007/s00418-008-0541-5

Zeisberg, E.M., O. Tarnavski, M. Zeisberg, A.L. Dorfman, J.R. McMullen, E. Gustafsson, A. Chandraker, X. Yuan, W.T. Pu, A.B. Roberts, et al. 2007. Endothelial-to-mesenchymal transition contributes to cardiac fibrosis. *Nat. Med.* 13:952–961. https://doi.org/10.1038/nm1613